

Grables: Tabular Learning Beyond Independent Rows

Tamara Cucumides¹ Floris Geerts¹

Abstract

Tabular learning is still dominated by row-wise predictors that score each row independently, which fits i.i.d. benchmarks but fails on transactional, temporal, and relational tables where labels depend on other rows. We show that row-wise prediction rules out natural targets driven by global counts, overlaps, and relational patterns. To make “using structure” precise across architectures, we introduce *grables*: a modular interface that separates how a table is lifted to a graph (constructor) from how predictions are computed on that graph (node predictor), pinpointing where expressive power comes from. Experiments on synthetic tasks, transaction data, and a RelBench clinical-trials data confirm the predicted separations: message passing captures inter-row dependencies that row-local models miss, and hybrid approaches that explicitly extracts inter-row structure and feeds it to strong tabular learners yield consistent gains.

1. Introduction

Tabular data underlies a large fraction of real-world machine learning, including applications in healthcare, finance, e-commerce, and the natural sciences. Despite sustained architectural progress, learning on tabular data remains dominated by a small class of highly optimized models, notably gradient-boosted decision trees (Chen & Guestrin, 2016; Ke et al., 2017; Prokhorenkova et al., 2018) and carefully tuned multilayer perceptrons (Gorishniy et al., 2025; Holzmüller et al., 2024). A common and largely implicit assumption shared by these methods is *row-locality*: predictions are made independently for each row, using only the attributes of that row, and are invariant to the presence, absence, or duplication of other rows in the table. This assumption aligns closely with standard i.i.d. benchmark constructions (Erickson et al., 2025) and helps explain the continued empirical

strength of row-wise predictors.

At the same time, many practically important tabular datasets violate this assumption. In transactional, temporal, and entity-centric tables, prediction targets often depend on relationships between rows, such as shared values, global counts, overlaps, or co-occurrence patterns. While such dependencies are routinely modelled in specialized settings, they remain underexplored in general-purpose tabular learning. Recent approaches, including graph-based models (Li et al., 2025) and transformer-style tabular foundation models that relax row-locality via cross-row interactions (Hollmann et al., 2025; Qu et al., 2025; Ma et al., 2025), report gains that are difficult to interpret: it is often unclear whether they reflect principled representational advantages or increased capacity or optimization effects.

This motivates a fundamental question: when does modelling inter-row structure provide a genuine advantage over row-local prediction, and what precisely enables that advantage? *Our answer is that this advantage is fundamentally representational: certain natural, extension-sensitive targets are inaccessible to any row-local predictor, regardless of model capacity.* To make this precise, we introduce *grables*, a modular interface that separates how a table is lifted to a relational structure from how predictions are computed on that structure. A grable consists of a *graph constructor*, which maps a table to a graph while preserving a canonical correspondence between rows and nodes, and a *node predictor*, which operates on the resulting graph. This abstraction makes explicit where structural inductive bias enters and provides a common language to compare row-wise tabular models, message-passing neural networks, and transformer-style tabular methods whose structure is implicit in attention.

Building on this interface, we formalize *grabular expressibility*, an expressiveness framework that characterizes which row-level prediction functions can be realized by a given family of constructors and predictors. Unlike standard neural network analyses (Barceló et al., 2020; Morris et al., 2019), which fix the input graph, our framework quantifies the families of graph views induced from the same underlying table. Using this lens, we show that row-local predictors are exactly those that are invariant under table extensions and therefore incapable of representing natural inter-row

¹Department of Computer Science, University of Antwerp, Belgium. Correspondence to: Tamara Cucumides <tamara.cucumidesfaundez@uantwerp.be>.

targets driven by counts, overlaps, or shared witnesses. In contrast, message-passing models that operate on simple, schema-driven constructions such as incidence graphs can represent such targets, but only up to well-defined limits that can be characterized using logical tools.

We complement this analysis with controlled experiments on synthetic and real transactional data that isolate extension-sensitive dependencies. These experiments empirically validate the predicted separations and show that apparent gains by row-local models—including strong tabular baselines and tabular foundation models—can arise from row-local cues rather than genuine relational reasoning. Finally, through a case study on a relational benchmark, we show that explicitly exposing inter-row structure and combining it with strong tabular representations yields consistent improvements, demonstrating that tabular and graph-based representations are complementary rather than competing.

See Appendix A for a detailed discussion of related work.

1.1. Background

We first provide the necessary background on tables, graphs, MPNNs, row, node and logic-based predictors.

Notation For sets X, Y , let $Y^X := \{f \mid f : X \rightarrow Y\}$, that is, X^Y is the set of all functions from X to Y .

Tables and row predictors Let \mathcal{C} be a (possibly infinite) universe of *column names* and let \mathbf{val} be a *value domain*. A *schema* is a finite set $C \subseteq \mathcal{C}$ of column names. For simplicity, we assume that every column $c \in \mathcal{C}$ takes values in \mathbf{val} . A *C-row* is a function $r : C \rightarrow \mathbf{val}$ (equivalently, an element of \mathbf{val}^C). A *C-table* is a finite set $T \subseteq \mathbf{val}^C$ of *C-rows*. When C is clear from context, we simply say *row* and *table*.

A *row predictor* is a function rpred that maps each pair (C, T) to a *per-row classifier* $\text{rpred}_{C, T} : T \rightarrow \{0, 1\} : r \mapsto \text{rpred}_{C, T}(r)$.

Graphs and node predictors A *graph* is a tuple $G = (V, E_1, \dots, E_m, \rho)$, where V is a finite set of nodes, each $E_i \subseteq V \times V$ is a (directed) edge relation (undirected edges are modelled by including both directions), and ρ assigns *row-valued features* to nodes. Formally, each node $v \in V$ carries a finite *local schema* $C(v) \subseteq \mathcal{C}$ and a feature row $\rho(v) \in \mathbf{val}^{C(v)}$. Thus nodes may have different local schemas. We let $N_i(v)$ consist of all vertices adjacent to v along E_i -edges.

A *node predictor* is a function npred that assigns to each graph G a (possibly partial) node classifier $\text{npred}_G : \text{npred}_G \rightarrow \{0, 1\} : v \mapsto \text{npred}_G(v)$.

MPNNs induce node predictors Fix a graph $G = (V, E_1, \dots, E_m, \rho)$. A *k-layer (heterogeneous) Message-Passing Neural Network* (MPNN) computes *node embeddings* $\mathbf{h}_v^{(\ell)} \in \mathbb{R}^d$ for $\ell = 0, \dots, k$, initialized from the node information $\rho(v)$ (and optional type $C(v)$), and updated for k rounds by permutation-invariant aggregation of messages from neighbours (per edge type) (Gilmer et al., 2017; Schlichtkrull et al., 2018). The final embedding is denoted by $\mathbf{h}_v^{(k)}$, for $v \in V$. These embeddings induce a (total) *node classifier* via a learnable scalar readout and thresholding:

$$\text{npred}_G^{\text{MPNN}} : V \rightarrow \{0, 1\} : v \mapsto \mathbb{I}[\text{READ}(\mathbf{h}_v^{(k)}) > 0],$$

where $\text{READ} : \mathbb{R}^d \rightarrow \mathbb{R}$ is learnable and $\mathbb{I}[\cdot]$ is the indicator. Since MPNNs are standard we defer details to Appendix B.

FO \cap MPNN node classifiers. A *k-layer MPNN* predicts a node label via k rounds of neighbourhood aggregation, hence depends only on the node’s k -hop neighbourhood. To formalize this locality, we relate MPNNs to *logic-defined* node queries: First-order logic (FO) is a broad language for specifying unary properties on graphs, while graded modal logic (GML) captures neighbourhood reasoning with thresholded counts. We write $\text{GML}^{(\leq k)}$ for the fragment of GML of *modal depth at most k*, i.e., formulas that nest the neighbourhood modalities at most k times. The following theorem makes this precise: among unary FO-definable classifiers, those realizable by *k*-layer MPNNs are exactly the queries definable in $\text{GML}^{(\leq k)}$.

Theorem 1.1 (Barceló et al. (2020)). *Fix $k \in \mathbb{N}$ and a unary FO formula $\varphi(x)$ over a graph schema σ_G representing graphs. The following are equivalent:*

1. φ is realized by some *k*-layer MPNN node classifier, i.e., $\text{npred}_G^{\text{MPNN}}(v) = 1 \iff G \models \varphi(v)$ for all G, v .
2. φ is equivalent to some $\psi(x) \in \text{GML}^{(\leq k)}$, i.e., $G \models \varphi(v) \iff G \models \psi(v)$ for all G, v .

Here $G \models \varphi(v)$ means that the graph G satisfies the property expressed by φ when the free variable is interpreted as node v . For example, the property “a node has a neighbour with the same label” is definable in GML (already at modal depth 1), and therefore can be realized by a 1-layer MPNN. Formal definitions are deferred to Appendix B.

2. Grables: A unifying interface for tabular and graph learning

As mentioned in the Introduction, tabular prediction sits at an awkward crossroads. Classical tabular methods (e.g., gradient-boosted trees) operate *directly* on rows and columns and typically expose no explicit relational structure beyond what is manually engineered. At the other extreme, relational and graph-based models *start* from an

explicit graph and learn over its neighbourhoods. Recent transformer-style tabular models (e.g., TabPFN) further blur the picture: they may capture rich interactions between cells (column/value pairs) and rows, but the induced “structure” lives implicitly in attention and is therefore hard to compare across architectures. This raises a basic question: *what does it even mean to compare the expressive power of methods that (i) see only rows, (ii) see an explicit graph, or (iii) induce structure implicitly?*

We address this by making the missing object explicit. We separate (a) *how a table is turned into a relational structure* from (b) *how predictions are computed on that structure*. The key abstraction is a *graph constructor* γ that equips each table with a graph representation while preserving a canonical correspondence between rows and nodes.

2.1. Grables

Let C be a schema and T a C -table. A *graph constructor* γ maps each pair (C, T) to a *graph* $G_{C,T}^\gamma = (V, E_1, \dots, E_m, \rho)$. Crucially, $G_{C,T}^\gamma$ contains one distinguished node for each row $r \in T$; we denote it by v_r and call it the *row node*. Row nodes store the row itself as features: $\rho(v_r) = r \in \text{val}^C$. Beyond row nodes, γ may introduce auxiliary nodes (e.g., values, column identifiers, join keys), edge relations, and additional features. We call any graph obtained from a table in this way a *grable*.¹

We give two natural examples. The first is the trivial grable: a graph encoding of a table, without any edges.

Example 2.1 (Trivial grable). For any schema C and C -table T , the *trivial grable* of (C, T) is the graph $G_{C,T}^{\text{triv}} = (V, E, \rho)$ where $V = \{v_r \mid r \in T\}$, $E = \emptyset$, and $\rho(v_r) = r$ for all $r \in T$. We write γ_{triv} for the corresponding constructor. \blacktriangleleft

The second example is the standard incidence encoding of tables, used for example in Grohe (2020) to assess the expressive power of MPNNs on relational data.

Example 2.2 (Incidence grable). Fix a schema $C \subseteq \mathcal{C}$ and an C -table T , and write $C = \{c_1, \dots, c_m\}$. The *incidence grable* of (C, T) is the graph $G_{C,T}^{\text{inc}} = (V, E_1, \dots, E_m, \rho)$ defined as follows.

- $V = V_{\text{row}} \cup V_{\text{val}}$, where $V_{\text{row}} = \{v_r \mid r \in T\}$ are the row nodes and $V_{\text{val}} = \{u_{i,a} \mid i \in [m], v \in \text{val}, \exists r \in T : r[c_i] = a\}$ contains one *value node* for each column–value pair that occurs in T .
- For each $i \in [m]$, the edge relation $E_i \subseteq V^2$ is given by $(v_r, u_{i,a}) \in E_i$ iff $r[c_i] = a$ (optionally also adding $(u_{i,a}, v_r)$ to make edges undirected).
- Row nodes store full rows, $\rho(v_r) = r \in \text{val}^C$; value nodes may store their value (and optionally the col-

¹We choose Grable=graph+table; Tabphs=table+graph does not sound well ;-)

umn), e.g. $\rho(u_{i,a})(c_i) = a$.

We write γ_{inc} for the corresponding constructor. \blacktriangleleft

We can also formalize grables corresponding to prominent transformer-style tabular models, including TabPFN (Hollmann et al., 2025) as well as CARTE (Kim et al., 2024) and TARTE (Kim et al., 2025), by making their tokenization and attention patterns explicit as graph constructors. We also consider Neighbourhood Feature Aggregation (NFA) (Bazhenov et al., 2025), which is a *derived* constructor: it requires a starting grable $G_{C,T}^\gamma$ to define 1-hop neighbourhoods, but its output is a *trivial grable* so that downstream learners can be purely tabular. See Appendix C for details.

2.2. Grabular expressiveness

Grables let us put tabular, relational, and transformer-style models on the same axis. The crucial point is that, for tables, there is *no single given graph*: the model must first *choose a view* of the table as a graph structure, and only then compute predictions. This yields a two-part inductive bias:

- a *constructor* γ that decides *what structure the model is allowed to use* (which nodes/edges/features), and
- a *node predictor* npred that decides *how predictions are computed* on that structure.

This separation is exactly what is missing when comparing (i) classical tabular methods that “see only rows”, (ii) graph (and also relational) models that start from an explicit neighbourhood structure, and (iii) transformer-style tabular models whose structure is implicit in attention. We propose an expressiveness notion makes these differences transparent: it attributes power either to a *stronger graph view* or to a *stronger predictor on a fixed view*.

Let Γ be a set of admissible graph constructors and let \mathcal{P} be a class of node predictors.

Definition 2.3 (Grabular expressibility). A row predictor rpred is (Γ, \mathcal{P}) -expressible if there exist a constructor $\gamma \in \Gamma$ and a node predictor $\text{npred} \in \mathcal{P}$ such that for *all* schemas C , all C -tables T , and all rows $r \in T$,

$$\text{rpred}_{C,T}(r) = \text{npred}_{G_{C,T}^\gamma}(v_r),$$

where v_r denotes the distinguished row node corresponding to r in the grable $G_{C,T}^\gamma$.

Equivalently, rpred is expressible if there is a *single, uniform* way to turn every table into a graph (using some $\gamma \in \Gamma$) so that the desired row-level decision reduces to a node-level decision on row nodes. We write $\text{Expr}(\Gamma, \mathcal{P}) := \{\text{rpred} \mid \text{rpred} \text{ is } (\Gamma, \mathcal{P})\text{-expressible}\}$ for the resulting expressiveness class. Importantly, we can now compare models by set inclusion: (Γ, \mathcal{P}) is (weakly) at least as expressive as (Γ', \mathcal{P}') if $\text{Expr}(\Gamma', \mathcal{P}') \subseteq \text{Expr}(\Gamma, \mathcal{P})$, etc.

Why this differs from standard graph expressiveness. Expressiveness results for MPNNs and graph logics typically fix the input graph G and study what a predictor can compute on that graph. In contrast, Definition 2.3 quantifies over a family of graph views of the same underlying object, that is, a table.

Why restrictions matter. Without restrictions on Γ and \mathcal{P} , the definition becomes vacuous: with γ_{triv} (isolated row nodes with $\rho(v_r) = r$) and an unconstrained npred , one can hard-code any $\text{rpred}_{C,T}$. We thus only obtain meaningful insights by fixing natural constructor families Γ (e.g. incidence, CARTE/TARTE-style graphlets, attention-induced graphs) and natural predictor classes \mathcal{P} such as those expressible by MPNNs.

3. Separations: when structure helps, and when message passing fails

In what follows, we fix the predictor side to be k -layer MPNNs, i.e., $\mathcal{P} = \mathcal{P}_{\text{MPNN}}^{(k)}$, and ask how the choice of constructor family Γ shapes $\text{Expr}(\Gamma, \mathcal{P}_{\text{MPNN}}^{(k)})$. Proof details are in Appendix D.

3.1. Baseline: on the trivial grable, MPNNs are row-wise

The trivial constructor γ_{triv} maps (C, T) to the edgeless graph $G_{C,T}^{\text{triv}}$ with one node v_r per row $r \in T$ and node features $\rho(v_r) = r$. With no edges, message passing cannot transmit information between rows.

Proposition 3.1 (MPNNs on γ_{triv} are row-wise). Fix $k \in \mathbb{N}$. For any k -layer MPNN node classifier on $G_{C,T}^{\text{triv}}$, there exists a function $f : \text{val}^C \rightarrow \{0, 1\}$ (determined by the learned parameters) such that for all $r \in T$,

$$\text{npred}_{G_{C,T}^{\text{triv}}}^{\text{MPNN}}(v_r) = f(r).$$

In particular, the prediction for r depends only on the column values of r and not on the rest of T .

This motivates the standard tabular baseline notion: a row predictor is *extension-invariant* (or *row-local*) if its output on a row does not change when other rows are added or removed from the table.

Definition 3.2 (Row-locality / extension invariance). A row predictor rpred is *row-local* if for all (C, T) and $r \in T$, $\text{rpred}_{C,T}(r) = \text{rpred}_{C,\{r\}}(r)$, equivalently, if there exists $f : \text{val}^C \rightarrow \{0, 1\}$ with $\text{rpred}_{C,T}(r) = f(r)$ for all T and $r \in T$.

Classical tabular models such as XGBoost, random forests, and MLPs are row-local at inference: once trained, they implement a map $f(r)$ and do not depend on the rest of T . Also, CARTE and TARTE do not introduce cross-row

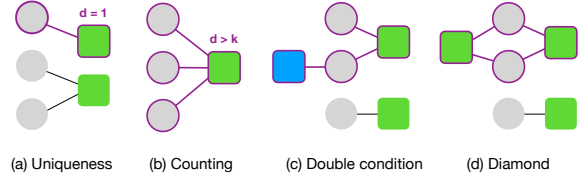


Figure 1. Incidence-grable patterns for our four tasks. Row nodes (circles) connect to column-value nodes (squares) via typed edges. (a) UNIQUE: a column-value node adjacent to a single row node. (b) COUNT: the degree of a shared column-value node. (c) DOUBLE: a length-3 pattern $v_r - u_{i,v} - v_s - u_{j,w}$ with a local constraint on v_s . (d) DIAMOND: two shared column-value nodes witnessing that the same row v_s overlaps twice with v_r .

connectivity: γ_{CARTE} builds a disjoint union of per-row star graphlets, and γ_{TARTE} connects only tokens within the same row (cfr. Appendix C). In contrast, any $(\Gamma, \mathcal{P}_{\text{MPNN}}^{(k)})$ with Γ containing constructors that create cross-row edges admits non-row-local predictors. For example, on the incidence grable, rows can exchange information through shared value nodes; and in TabPFN, column-wise attention enables cross-row information flow.

Remark (logical view). On $G_{C,T}^{\text{triv}}$ there are no edges, so graded modal operators are vacuous: any depth- k GML row property is equivalent (on row nodes) to a Boolean combination of unary predicates encoding the row’s own features. In particular, constant-depth MPNNs have exactly row-wise expressive power on γ_{triv} .

Takeaway. γ_{triv} is the exact baseline for row-wise tabular learning: on this constructor, every k -layer MPNN reduces to an independent per-row classifier.

3.2. Canonical inter-row structure: the incidence grable

To expose inter-row dependencies, we use the schema-driven incidence constructor γ_{inc} . It creates a row node v_r for each $r \in T$ and a value node $u_{i,v}$ for each occurring column-value pair (a_i, v) , with a typed edge $(v_r, u_{i,v}) \in E_i$ iff $r[a_i] = v$. This bipartite encoding makes “rows share values” relationships explicit to message passing.

Four minimal inter-row targets. We use four intentionally simple per-row predictors, illustrated in Figure 1: UNIQUE (a value appears only in r), COUNT $_N$ (at least N other rows share a designated value with r , with COUNT($=$) as the exactly N case), DOUBLE (*another* row shares a value with r and satisfies a local condition), and DIAMOND (there is a *another* row sharing two values with r).

We start by observing that these targets genuinely require inter-row information, and therefore lie outside the row-

local baseline captured by γ_{triv} .

Proposition 3.3 (Incidence separates row-locality). *Each predictor in Figure 1 is not row-local. Equivalently, none lies in $\text{Expr}(\{\gamma_{\text{triv}}\}, \mathcal{P})$ for any node-predictor class \mathcal{P} .*

On γ_{inc} , however, the first three tasks fall squarely within graded modal logic: they can be written as shallow GML formulas over the incidence signature (modal depth 2 for UNIQUE/COUNT_N, and depth 3 for DOUBLE). By Theorem 1.1 (FO \cap MPNN \Leftrightarrow GML), this immediately implies realizability by constant-depth MPNNs.

Proposition 3.4. *Let $\mathcal{P}_{\text{MPNN}}^{(k)}$ denote k-layer MPNNs. For the tasks in Figure 1(a–c),*

- UNIQUE, COUNT_N $\in \text{Expr}(\{\gamma_{\text{inc}}\}, \mathcal{P}_{\text{MPNN}}^{(2)})$,
- DOUBLE $\in \text{Expr}(\{\gamma_{\text{inc}}\}, \mathcal{P}_{\text{MPNN}}^{(3)})$.

The remaining task, DIAMOND, is the first point where one must *bind a shared witness*: the same other row must simultaneously witness two overlaps with r (Figure 1(d)). This is FO-definable on the incidence graph, but Theorem 1.1 implies that no bounded-depth MPNN can express it.

Proposition 3.5 (Diamond is beyond MPNNs on incidence grable). *For every $k \in \mathbb{N}$,*

$$\text{DIAMOND} \notin \text{Expr}(\{\gamma_{\text{inc}}\}, \mathcal{P}_{\text{MPNN}}^{(k)}).$$

Takeaway. Incidence gives a principled “relational lift” of tables: it strictly enlarges what is learnable beyond row-local tabular baselines, yet logic still certifies a clean expressiveness gap for message passing. One can, however, also see this as a limitation of the *constructor* rather than of message passing. In Appendix D we give a simple *extension* of the incidence grable under which DIAMOND becomes definable in shallow GML and therefore MPNN-expressible.

3.3. MPNNs on NFA: graph power compiled into feature width

Neighbourhood Feature Aggregation (NFA) is *derived* from a base constructor γ : it first builds a grable $G_{C,T}^{\gamma}$ to define 1-hop neighbourhoods, computes a fixed menu of local aggregates around each row node, and then *discards the graph* by outputting the trivial grable $G_{C,T}^{\text{NFA}} = (V_{\text{row}}, \emptyset, \rho^{\text{NFA}})$ (see Appendix C.4).

As a result, any predictor applied *after* NFA is graph-agnostic and can access inter-row information only through the compiled features ρ^{NFA} (e.g., counts and simple statistics such as min / max / mean, one-hot means). This makes NFA effective for shallow relational signals, but deeper patterns must be compiled by iterating augmentations or adding channels: on an incidence-style base graph with k typed attribute edges, the number of distinct typed L -step interaction patterns grows as k^L , so preserving the information

available after L rounds of typed message passing can require exponentially many aggregate channels. This limits the effectiveness of NFA for deeper relational patterns.

4. Experiments and results

Our theory isolates two distinct sources of inductive bias in tabular pipelines: (i) the representation induced by the table-to-graph constructor, and (ii) the downstream predictor class. Section 3 then translates this into concrete expressiveness gaps, showing when row-local predictors (extension-invariant by design) cannot realize targets that depend on relationships between rows. Our experiments ² are not designed to demonstrate state-of-the-art performance, but to test whether these theoretical bottlenecks appear empirically under progressively more realistic conditions. Rather than treating graph-based models as generic alternatives to tabular methods, we use them as controlled interventions: we ask when row-local representations are structurally misaligned with the target, and whether exposing cross-row structure via explicit constructions and message passing resolves that mismatch.

We organize our experiments around three questions:

(Q1) *Can the representational separation between row-local models and message-passing models be observed in practice under controlled conditions?* We begin with synthetic data and tasks that isolate extension-sensitive dependencies, allowing us to directly test the theoretical distinctions introduced in the previous sections.

(Q2) *Does the same separation arise on real-world tabular data when the prediction task depends on cross-row structure?* We then move to real data while retaining tasks that explicitly depend on relationships between rows, enabling us to examine whether the same failure modes persist outside of hand-crafted settings.

(Q3) *Can the information coming from the graph structure be combined with strong tabular models to lift their structural limitations and how does this affect their performance?* Finally, we move to a case study where tabular models show good results and see if feeding them cross-row aware information improves their performance

Across all three settings, the experiments are designed to elucidate the role of representation rather than optimize performance. By progressively increasing complexity while keeping the underlying structural question fixed, the empirical results provide a coherent picture of when and why modeling cross-row structure matters in tabular learning.

²Code available at: <https://github.com/TamaraCucumides/Grables>

4.1. Experimental setup

Datasets. We focus on three data settings, each one aimed at each one of our experimental research questions. Statistics and details can be found in Appendix F.1

1. **Synthetic dataset.** A transactions dataset with four categorical features.
2. **Transaction dataset.** A real-world dataset derived from retail transactions, in which inter-row dependencies arise naturally (Chen, 2015).
3. **Clinical trials dataset.** For our case study, we consider the clinical trials dataset `relbench-trial` from the Relbench benchmark (Robinson et al., 2024).

We deliberately avoid both generic tabular and graph benchmarks. Generic tabular benchmarks are typically curated under i.i.d. assumptions that align closely with row-local learning and therefore do not stress the representational limitations studied in this work. Graph benchmarks, by contrast, presuppose explicit structure and prediction targets that favor structural models by construction.

Tasks and leakage control. We instantiate the four logical tasks introduced in Section 3 on the synthetic and transaction datasets. To prevent information leakage, tasks are generated *independently within each split*, using disjoint train/validation/test partitions (90/10/10). When graph representations are used, a separate graph is constructed per split and all learning is performed in an inductive setting. For the `relbench-trial` dataset, we follow the standard RelBench protocol and predefined splits. Full task-generation details are provided in Appendix F.2.

Models. We consider three modeling paradigms. For row-local tabular learning, we include gradient-boosted decision trees (LightGBM (Ke et al., 2017)), neural networks (realMLP (Holzmüller et al., 2024)), and a tabular foundation model (TabPFN). These serve as strong, up-to-date baselines that perform consistently well across recent tabular benchmarks, including the living benchmark TabArena (Erickson et al., 2025). LightGBM and realMLP are tuned using AutoGluon (Erickson et al., 2020), while TabPFN (version 2.5) is used following its documentation.

For graph-based learning on table-derived structure, we use heterogeneous graph neural networks, represented by HeteroSage (Hamilton et al., 2017), operating on the incidence graph. In the relational case study, we additionally include established relational models: relational deep learning (RDL (Robinson et al., 2024)), relational graph transformers (RGT (Dwivedi et al., 2025)), and a relational foundation model (KumoRFM (Fey et al., 2025)).

Architectural details, hyperparameters, and training protocols are reported in Appendices F.3, F.4 and F.5.

Evaluation metrics. Across all experiments, performance is measured using the area under the receiver operating characteristic curve (ROC–AUC). Because the logical tasks naturally induce class imbalance, we additionally report F1 scores where appropriate.

4.2. Results on synthetic data

Table 1 reports performance on the logical tasks. On UNIQUE and COUNT, the GNN strongly outperforms tabular models and TabPFN, achieving near-perfect scores. The equality variant of COUNT is harder due to its finer decision boundary, explaining the modest performance drop despite extended training (Appendix F.5).

On DOUBLE and DIAMOND, GNN performance is comparable to tabular baselines and TabPFN. However, several tabular models achieve elevated scores despite lacking access to cross-row structure (notably realMLP on COUNT(>), DOUBLE, and DIAMOND, and LightGBM on COUNT(=), DOUBLE, and DIAMOND), indicating the presence of row-local shortcuts. We first probe the robustness of these effects via a sensitivity analysis based on controlled perturbations of the test set, which yields similar behavior (Appendix G.1.1).

To distinguish shortcut learning from genuine relational reasoning, we introduce a stress-test dataset that suppresses row-local cues. As shown in Figure 2, the elevated validation and test performance of tabular models collapses on the stress set (Appendix G.1.2), indicating that these gains do not reflect the intended dependencies. The same effect is observed for the GNN on DIAMOND, which is structurally inaccessible under the incidence graph (Proposition 3.5).

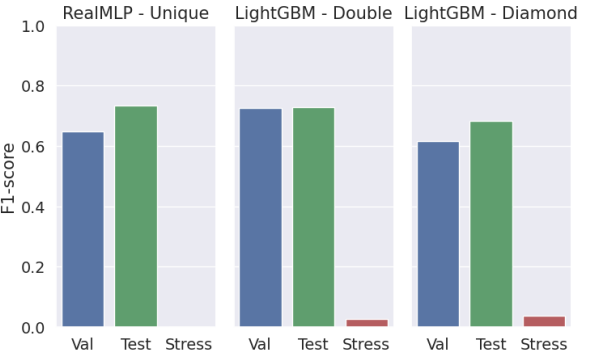


Figure 2. F1-score in validation, test and stress data of RealMLP in Unique, and LightGBM in Double and Diamond tasks.

Finally, while TabPFN has implicit access to cross-row interactions, it consistently underperforms the GNN. Taken together, these results empirically confirm the representational separation predicted by our analysis: under controlled

Table 1. Results on logical tasks across synthetic and transaction datasets. For each task we report metric AUC and F1. Cases where tabular models get a 0.0 F1-score correspond to cases where the models predict 0 for all instances.

Model	UNIQUE		COUNT		COUNT(=)		DOUBLE		DIAMOND	
	AUC	F1-score								
Transactions synthetic data										
LightGBM	0.566	0.123	0.889	0.000	0.675	0.314	0.789	0.729	0.846	0.682
realMLP	0.516	0.123	0.933	0.733	0.521	0.000	0.785	0.686	0.796	0.603
TabPFN2.5	0.823	0.025	0.962	0.775	0.340	0.055	0.670	0.699	0.868	0.702
GNN (Sage)	0.997	0.986	1.000	1.000	0.988	0.859	0.887	0.777	0.899	0.676
Transactions real data (retail)										
LightGBM	0.570	0.190	0.500	0.000	0.500	0.027	0.847	0.815	0.821	0.199
RealMLP	0.853	0.190	0.929	0.881	0.477	0.027	0.703	0.000	0.792	0.139
TabPFN2.5	0.793	0.404	0.827	0.001	0.758	0.023	0.463	0.003	0.659	0.007
GNN (Sage)	0.998	0.988	0.999	0.967	0.903	0.171	0.910	0.863	0.807	0.251

conditions, only models with explicit message passing reliably capture extension-sensitive relational targets.

4.3. Results on retail transactions data

Results on the retail transactions dataset largely mirror those observed on synthetic data. For UNIQUE and COUNT, the GNN consistently outperforms both tabular models and TabPFN, indicating that the representational advantage conferred by explicit message passing persists beyond hand-crafted settings. For DOUBLE and DIAMOND, the gap narrows, but the GNN retains a systematic advantage.

The COUNT(=) task highlights an additional challenge introduced by real data. While this target is representationally accessible to the GNN, the presence of heterogeneous and task-irrelevant features hinders its ability to isolate the fine-grained decision boundary, leading to degraded performance. When this extraneous noise is reduced, the GNN recovers the expected behaviour (Appendix G.2.1).

Overall, these results answer (Q2) in the affirmative: the separation between row-local and message-passing models also arises on real-world tabular data, although its empirical expression depends on the model’s ability to disentangle relational signal from feature noise.

4.4. Case study: `relbench-trial`

We now turn to (Q3) and study whether inter-row structure can be combined with tabular models to overcome their inherent row-local limitations. We focus on the `relbench-trial` dataset from the RelBench benchmark, a relational learning setting that behaves atypically: unlike other RelBench tasks, it consistently favours strong tabular models operating on a single table over graph-based

models trained on the full relational entity graph.³

This case study serves two purposes. First, it helps explain why purely relational models underperform on `relbench-trial`. Second, it allows us to test whether exposing inter-row structure—while retaining the strengths of tabular learning—can yield systematic improvements, as predicted by the analysis in Section 3.2.

Baselines: tabular and relational graph models. Table 2 reports validation and test ROC–AUC scores. Consistent with prior work, a strong tabular baseline (LightGBM) outperforms graph-based models trained on the relational entity graph (RDL, RGT) and is competitive with the relational foundation model KumoRFM. This suggests that much of the predictive signal for this dataset is concentrated within the target table rather than distributed across the database.

However, purely tabular predictors remain row-local and are therefore blind to dependencies between rows of the same table, even when such dependencies are predictive, which leads to a possible alternative: hybrid models.

Hybrid models: combining tabular learning with inter-row structure. To address this limitation, we augment the tabular model with representations that expose inter-row dependencies. We consider two complementary mechanisms. First, we use a time-aware *tabular neighbourhood feature aggregation*, which compiles one-hop inter-row statistics from the incidence graph into explicit features (Appendix E). Second, we use *learned message-passing representations*, obtained from GNNs operating on (i) the incidence graph (Tab+GNN(T)), (ii) the relational entity graph

³The relational entity graph consist of trivial grables, one for each table, and where row nodes are connected based on key/foreign key constraints. It can also be seen as a grable.

Table 2. Performance comparison (AUC) on `relbench-trial`. Results from RDL, RGT and KumoRFM are taken from their respective papers. KumoRFM does not report validation scores. Results are averaged over 5 runs.

Model	val-auc	test-auc
LightGBM	0.6830	0.7009
RDL (GNN)	0.6818	0.6860
RGT (Graph Transformer)	0.6678	0.6861
KumoRFM	–	0.7079
KumoRFM (finetuned)	–	0.7116
GNN(T)	0.6837	0.7151
Tab+NFA(T)	0.7024	0.7254
Tab+GNN(T)	0.7011	0.7241
Tab+GNN(DB)	0.6936	0.7180
Tab+GNN(T+DB)	0.7214	0.7486

(Tab+GNN(DB)), and (iii) both jointly (Tab+GNN(T+DB)). In all cases, the resulting structural features—whether fixed or learned—are concatenated with the original tabular attributes rather than replacing them.⁴

Across all hybrid variants, we observe a consistent performance gain over the purely tabular model, the graph-based models, and the relational foundation model (Table 4.4). This confirms that explicitly exposing structure—whether through fixed aggregations or learned message passing—can lift the structural limitations of row-local learning when combined with a strong tabular predictor.

Do tabular predictors use the learned structure? We analyze permutation-based feature importance. Across all hybrid models, GNN-derived embeddings dominate the top-ranked features: 7 of the top-15 for Tab+GNN(DB) and 9 for Tab+GNN(T). This shows that the tabular learner relies on message-passing representations even in the presence of strong row-local features (Appendix G.3.1).

Do different sources of structure lead to different predictions? Although Tab+GNN(T) and Tab+GNN(DB) achieve similar ROC–AUC scores, their predictions are not identical. Figure 3 shows that while the models agree on most instances, a non-trivial subset of predictions differs (125 out of 825, about 15%). This reflects the distinct inductive biases induced by inter-row structure within the table versus relational structure across tables, with each representation proving beneficial for different subsets of samples.

Taken together, these results answer (Q3) in the affirmative. While strong tabular models capture most of the predictive

⁴The original RelBench study also considers feeding GNN embeddings into LightGBM. In that setting, the tabular features are omitted, which does not improve over the purely tabular LightGBM. Our setup differs in that we retain the original tabular features and treat graph-based representations as complementary, rather than substitutive sources of information.

Predictions overlap between models

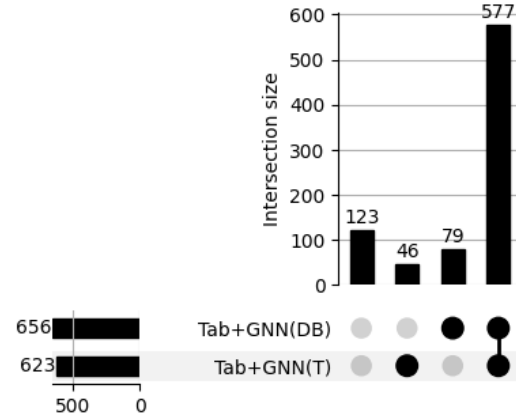


Figure 3. UpSet plot showing the overlap and disagreement predictions between model predictions in the test set.

signal in `relbench-trial`, augmenting them with explicitly extracted inter-row and relational structure—via either fixed aggregations or learned message passing—yields consistent, non-redundant improvements. This demonstrates that tabular and graph-based representations are complementary rather than competing, and motivates hybrid, structure-aware tabular learning as a principled way to overcome row-local limitations.

5. Conclusions

We examined the expressive limits of row-wise prediction in tabular learning and showed that treating rows independently rules out targets whose values depend on relationships between rows. Through controlled experiments on synthetic and real tabular and relational data, we demonstrated that these limitations manifest in practice. Models with access to explicit inter-row structure capture extension-sensitive dependencies that row-local predictors miss, while strong tabular models benefit when such structure is exposed in a form they can exploit. These results highlight that tabular and graph-based methods are complementary, not competing.

Limitations. Introducing structure increases computational cost and is not universally beneficial, and different tasks may require different structural views that are not always evident *a priori*. Our analysis focuses on a limited class of constructions and targets, and extending it to adaptive or end-to-end structure selection remains an open problem. For clarity of exposition, both the theory and experiments are instantiated in a binary classification setting. This choice simplifies definitions and notation and is not a fundamental restriction: the proposed framework and expressiveness analysis extend to multiclass classification and regression.

Impact Statement

This paper presents work whose primary goal is to advance the understanding of representational limitations in tabular machine learning and to provide a principled framework for reasoning about when and why modeling inter-row structure is beneficial. The contributions are methodological and theoretical in nature, focusing on expressiveness, inductive bias, and experimental diagnosis rather than on deploying new predictive systems.

By clarifying when row-local tabular models are structurally misaligned with the prediction task, this work may help practitioners avoid inappropriate model choices in settings such as transactional, temporal, or relational data. This could have positive downstream effects by encouraging more reliable modeling practices in application domains where tabular data is prevalent, including science, healthcare, and industry. At the same time, the work does not introduce new data sources, new deployment scenarios, or new mechanisms for decision-making about individuals.

The techniques and analyses presented here do not raise novel ethical concerns beyond those commonly associated with machine learning research on tabular data. As with any modeling approach, improper use on sensitive data or in high-stakes decision-making contexts may carry risks, but these risks are not specific to the framework proposed in this paper.

References

Impact Statement

This paper presents work whose primary goal is to advance the understanding of representational limitations in tabular machine learning and to provide a principled framework for reasoning about when and why modeling inter-row structure is beneficial. The contributions are methodological and theoretical in nature, focusing on expressiveness, inductive bias, and experimental diagnosis rather than on deploying new predictive systems.

By clarifying when row-local tabular models are structurally misaligned with the prediction task, this work may help practitioners avoid inappropriate model choices in settings such as transactional, temporal, or relational data. This could have positive downstream effects by encouraging more reliable modeling practices in application domains where tabular data is prevalent, including science, healthcare, and industry. At the same time, the work does not introduce new data sources, new deployment scenarios, or new mechanisms for decision-making about individuals.

The techniques and analyses presented here do not raise novel ethical concerns beyond those commonly associated with machine learning research on tabular data. As with any modeling approach, improper use on sensitive data or in high-stakes decision-making contexts may carry risks, but these risks are not specific to the framework proposed in this paper.

References

Anonymous. Fixed aggregation features can rival GNNs. In *Submitted to The Fourteenth International Conference on Learning Representations*, 2025. URL <https://openreview.net/forum?id=A8Ju0tpAUM>. under review.

Badaro, G., Saeed, M., and Papotti, P. Transformers for tabular data representation: A survey of models and applications. *Transactions of the Association for Computational Linguistics*, 11:227–249, 03 2023. ISSN 2307-387X. doi: 10.1162/tacl_a_00544. URL https://doi.org/10.1162/tacl_a_00544.

Barceló, P., Kostylev, E. V., Monet, M., Pérez, J., Reutter, J. L., and Silva, J. P. The logical expressiveness of graph neural networks. In *International Conference on Learning Representations*, 2020. URL <https://openreview.net/pdf?id=r11Z7AEKvB>.

Bazhenov, G., Platonov, O., and Prokhorenko, L. Graphland: Evaluating graph machine learning models on diverse industrial data. In *The Thirty-ninth Annual Conference on Neural Information Processing Systems Datasets and Benchmarks Track*, 2025. URL <https://openreview.net/forum?id=Gyq8lMqdk5>.

Chen, D. Online Retail. UCI Machine Learning Repository, 2015. DOI: <https://doi.org/10.24432/C5BW33>.

Chen, T. and Guestrin, C. Xgboost: A scalable tree boosting system. KDD '16, pp. 785–794, New York, NY, USA, 2016. Association for Computing Machinery. ISBN 9781450342322. doi: 10.1145/2939672.2939785. URL <https://doi.org/10.1145/2939672.2939785>.

Cucumides, T. and Geerts, F. From features to structure: Task-aware graph construction for relational and tabular learning with gnns. *arXiv preprint arXiv:2506.02243*, 2025.

Dwivedi, V. P., Jaladi, S., Shen, Y., López, F., Kanatsoulis, C. I., Puri, R., Fey, M., and Leskovec, J. Relational graph transformer. *arXiv preprint arXiv:2505.10960*, 2025.

Erickson, N., Mueller, J., Shirkov, A., Zhang, H., Larroy, P., Li, M., and Smola, A. Autogluon-tabular: Robust and accurate automl for structured data. *arXiv preprint arXiv:2003.06505*, 2020.

Erickson, N., Purucker, L., Tschalzhev, A., Holzmüller, D., Desai, P. M., Salinas, D., and Hutter, F. Tabarena: A living benchmark for machine learning on tabular data. *arXiv preprint arXiv:2506.16791*, 2025. URL <https://arxiv.org/abs/2506.16791>.

Fey, M., Hu, W., Huang, K., Lenssen, J. E., Ranjan, R., Robinson, J., Ying, R., You, J., and Leskovec, J. Position: Relational deep learning - graph representation learning on relational databases. In Salakhutdinov, R., Kolter, Z., Heller, K., Weller, A., Oliver, N., Scarlett, J., and Berkenkamp, F. (eds.), *Proceedings of the 41st International Conference on Machine Learning*, volume 235 of *Proceedings of Machine Learning Research*, pp. 13592–13607. PMLR, 21–27 Jul 2024. URL <https://proceedings.mlr.press/v235/fey24a.html>.

Fey, M., Kocijan, V., Lopez, F., Lenssen, J., and Leskovec, J. Kumorfm: A foundation model for in-context learning on relational data, 2025.

Gilmer, J., Schoenholz, S. S., Riley, P. F., Vinyals, O., and Dahl, G. E. Neural message passing for quantum chemistry. In *Proceedings of the 34th International Conference on Machine Learning - Volume 70*, ICML'17, pp. 1263–1272. JMLR.org, 2017. URL <https://dl.acm.org/doi/10.5555/3305381.3305512>.

Gorishniy, Y., Rubachev, I., Khrulkov, V., and Babenko, A. Revisiting deep learning models for tabular data. In Ranzato, M., Beygelzimer, A., Dauphin, Y., Liang, P., and Vaughan, J. W. (eds.), *Advances in Neural Information Processing Systems*, volume 34, pp. 18932–18943. Curran Associates, Inc., 2021. URL <https://openreview.net/forum?id=Gyq8lMqdk5>.

//proceedings.neurips.cc/paper_files/paper/2021/file/9d86d83f925f2149e9edb0ac3b49229c-Paper.pdf.

Gorishniy, Y., Kotelnikov, A., and Babenko, A. Tabm: Advancing tabular deep learning with parameter-efficient ensembling. In *The Thirteenth International Conference on Learning Representations*, 2025. URL <https://openreview.net/forum?id=Sd4wYYOhmY>.

Grinsztajn, L., Flöge, K., Key, O., Birkel, F., Jund, P., Roof, B., Jäger, B., Safaric, D., Alessi, S., Hayler, A., Manium, M., Yu, R., Jablonski, F., Hoo, S. B., Garg, A., Robertson, J., Bühler, M., Moroshan, V., Purucker, L., Cornu, C., Wehrhahn, L. C., Bonetto, A., Schölkopf, B., Gambhir, S., Hollmann, N., and Hutter, F. TabPFN-2.5: Advancing the state of the art in tabular foundation models, 2025. URL <https://arxiv.org/abs/2511.08667>.

Grohe, M. word2vec, node2vec, graph2vec, x2vec: Towards a theory of vector embeddings of structured data. In *Proceedings of the 39th ACM SIGMOD-SIGACT-SIGAI Symposium on Principles of Database Systems*, PODS’20, pp. 1–16. ACM, 2020. URL <https://doi.org/10.1145/3375395.3387641>.

Hamilton, W. L., Ying, R., and Leskovec, J. Inductive representation learning on large graphs. In *Advances in Neural Information Processing Systems*, volume 31, pp. 1025–1035, 2017. URL <https://dl.acm.org/pdf/10.5555/3294771.3294869>.

Hollmann, N., Müller, S., Purucker, L., Krishnakumar, A., Körfer, M., Hoo, S. B., Schirrmeister, R. T., and Hutter, F. Accurate predictions on small data with a tabular foundation model. *Nature*, 637(8045):319–326, 2025.

Holzmüller, D., Grinsztajn, L., and Steinwart, I. Better by default: Strong pre-tuned mlps and boosted trees on tabular data. In Globerson, A., Mackey, L., Belgrave, D., Fan, A., Paquet, U., Tomczak, J., and Zhang, C. (eds.), *Advances in Neural Information Processing Systems*, volume 37, pp. 26577–26658. Curran Associates, Inc., 2024. doi: 10.52202/079017-0837. URL https://proceedings.neurips.cc/paper_files/paper/2024/file/2ee1c87245956e3eaa71aaba5f5753eb-Paper-Conference.pdf.

Huang, X., Khetan, A., Cvitkovic, M., and Karnin, Z. Tab-transformer: Tabular data modeling using contextual embeddings, 2020. URL <https://arxiv.org/abs/2012.06678>.

Ke, G., Meng, Q., Finley, T., Wang, T., Chen, W., Ma, W., Ye, Q., and Liu, T.-Y. Lightgbm: A highly efficient gradient boosting decision tree. In Guyon, I., Luxburg, U. V., Bengio, S., Wallach, H., Fergus, R., Vishwanathan, S., and Garnett, R. (eds.), *Advances in Neural Information Processing Systems*, volume 30. Curran Associates, Inc., 2017. URL https://proceedings.neurips.cc/paper_files/paper/2017/file/6449f44a102fde848669bdd9eb6b76fa-Paper.pdf.

Kim, M. J., Grinsztajn, L., and Varoquaux, G. CARTE: Pretraining and transfer for tabular learning. In *Forty-first International Conference on Machine Learning*, 2024. URL <https://openreview.net/forum?id=9kArQnKLDP>.

Kim, M. J., Lefebvre, F., Brison, G., Perez-Lebel, A., and Varoquaux, G. Table foundation models: on knowledge pre-training for tabular learning. *Transactions on Machine Learning Research*, 2025. ISSN 2835-8856. URL <https://openreview.net/forum?id=QV4P8Csw17>.

LeDell, E., Poirier, S., et al. H2o automl: Scalable automatic machine learning. In *Proceedings of the AutoML Workshop at ICML*, volume 2020, pp. 24, 2020.

Li, C.-T., Tsai, Y.-C., Chen, C.-Y., and Liao, J. C. Graph neural networks for tabular data learning: A survey with taxonomy and directions. *ACM Comput. Surv.*, 58(1), September 2025. ISSN 0360-0300. doi: 10.1145/3744918. URL <https://doi.org/10.1145/3744918>.

Ma, J., Thomas, V., Hosseinzadeh, R., Labach, A., Cresswell, J. C., Golestan, K., Yu, G., Caterini, A. L., and Volkovs, M. TabDPT: Scaling tabular foundation models on real data. In *The Thirty-ninth Annual Conference on Neural Information Processing Systems*, 2025. URL <https://openreview.net/forum?id=pIZxE0ZCId>.

Morris, C., Ritzert, M., Fey, M., Hamilton, W. L., Lenssen, J. E., Rattan, G., and Grohe, M. Weisfeiler and leman go neural: Higher-order graph neural networks. *Proceedings of the AAAI Conference on Artificial Intelligence*, 33(01):4602–4609, Jul. 2019. doi: 10.1609/aaai.v33i01.33014602. URL <https://ojs.aaai.org/index.php/AAAI/article/view/4384>.

Prokhorenkova, L., Gusev, G., Vorobev, A., Dorogush, A. V., and Gulin, A. Catboost: unbiased boosting with categorical features. In Bengio, S., Wallach, H., Larochelle, H., Grauman, K., Cesa-Bianchi, N., and Garnett, R. (eds.), *Advances in Neural Information Processing Systems*, volume 31. Curran Associates, Inc., 2018. URL https://proceedings.neurips.cc/paper_files/paper/2018/file/14491b756b3a51daac41c24863285549-Paper.pdf.

Qu, J., Holzmüller, D., Varoquaux, G., and Morvan, M. L. TabICL: A tabular foundation model for in-context learn-

ing on large data. In *Forty-second International Conference on Machine Learning*, 2025. URL <https://openreview.net/forum?id=0VvD1PmNzM>.

Robinson, J., Ranjan, R., Hu, W., Huang, K., Han, J., Dobles, A., Fey, M., Lenssen, J. E., Yuan, Y., Zhang, Z., He, X., and Leskovec, J. Relbench: A benchmark for deep learning on relational databases. In Globerson, A., Mackey, L., Belgrave, D., Fan, A., Paquet, U., Tomczak, J., and Zhang, C. (eds.), *Advances in Neural Information Processing Systems*, volume 37, pp. 21330–21341. Curran Associates, Inc., 2024. doi: 10.52202/079017-0672. URL https://proceedings.neurips.cc/paper_files/paper/2024/file/25cd345233c65fac1fec0ce61d0f7836-Paper-Datasets_and_Benchmarks_Track.pdf.

Schlichtkrull, M., Kipf, T. N., Bloem, P., van den Berg, R., Titov, I., and Welling, M. Modeling relational data with graph convolutional networks. In *The Semantic Web*, pp. 593–607. Springer, 2018. URL https://doi.org/10.1007/978-3-319-93417-4_38.

Yang, C., Akimoto, Y., Kim, D. W., and Udell, M. Oboe: Collaborative filtering for automl model selection. KDD '19, pp. 1173–1183, New York, NY, USA, 2019. Association for Computing Machinery. ISBN 9781450362016. doi: 10.1145/3292500.3330909. URL <https://doi.org/10.1145/3292500.3330909>.

A. Related Work

Tabular learning. Learning on tabular data has been dominated by a set of highly effective model classes, including gradient-boosted decision trees (GBDTs) such as LightGBM, XGBoost, and CatBoost (Ke et al., 2017; Chen & Guestrin, 2016; Prokhorenkova et al., 2018), as well as carefully tuned multilayer perceptrons designed for tabular inputs, including RealMLP and TabM (Holzmüller et al., 2024; Gorishniy et al., 2025). These models form the basis of many practical systems and are commonly paired with AutoML tools for hyperparameter tuning, model selection, and ensembling (LeDell et al., 2020; Yang et al., 2019; Erickson et al., 2020).

A shared characteristic of these approaches is that predictions are defined at the level of individual rows, using only the attributes of the row itself. This modeling choice aligns naturally with i.i.d. benchmark formulations and has proven effective across a wide range of applications. This alignment is reinforced by common tabular benchmark protocols, which typically rely on random splits and implicitly assume i.i.d. data, even when this assumption may not strictly hold in practice (Erickson et al., 2025).

Our work departs from this setting by constructing prediction tasks whose targets depend on relationships between rows. Rather than modifying the underlying tabular architectures, we use these tasks to systematically probe how standard tabular models behave when the assumptions under which they are typically evaluated no longer hold, and to motivate the need for representations that can access inter-row information.

Transformer-based models for tabular data. A parallel line of work adapts transformer architectures to tabular inputs, motivated by the success of attention-based models in natural language processing. Models such as FT-Transformer (Gorishniy et al., 2021) and TabTransformer (Huang et al., 2020) primarily apply attention over features within a single row, and thus remain row-local at inference time. More broadly, transformer-based tabular models typically rely on serializing tables into token sequences and injecting structural bias through positional embeddings, masking schemes, or token-type indicators, rather than through explicit relational structure.

Recent surveys (Badaro et al., 2023) provide a comprehensive taxonomy of these design choices, covering table serialization strategies, positional encodings, and architectural adaptations. While such models may implicitly capture statistical regularities across rows through attention, the induced notion of structure depends on tokenization and architectural details and is not explicitly represented. As a result, it is difficult to characterize which inter-row dependencies these models can or cannot represent in principle, or to disentangle genuine relational reasoning from effects of model capacity or training data scale. Our work is complementary to this literature in that we introduce an explicit abstraction separating table-to-structure construction from prediction, enabling a principled analysis of when and why access to inter-row structure matters.

Tabular foundation models. Recent tabular foundation models such as TabPFN (Hollmann et al., 2025), TabICL (Qu et al., 2025), and TabDPT (Ma et al., 2025) leverage attention mechanisms to enable interactions between rows at inference time, thereby relaxing the row-locality assumption that underlies most traditional tabular predictors. The primary motivation of this line of work is to provide zero- or few-shot, ready-to-use models that generalize across a wide range of tabular datasets, rather than to explicitly study or characterize the structural limitations induced by row-local representations⁵. The link and difference between this line of work and ours is that we explicitly focus on inter-row structure and its representational consequences. Accordingly, we include in our experiments a representative tabular foundation model, TabPFN, which explicitly incorporates cross-row attention, and evaluate its behavior on tasks that require reasoning beyond row locality.

Graph learning over tabular data. Several works apply graph learning to tabular data by first transforming tables into graphs and then using message-passing models on the resulting structure. A recent survey (Li et al., 2025) systematizes these approaches and categorizes table-to-graph constructions, including graphs where rows are nodes connected by similarity or temporal relations, feature- or feature-value-centric constructions, and heterogeneous or bipartite graphs linking rows and attributes. Related work in relational deep learning extends this paradigm to multi-table databases, where rows correspond to entities in a relational entity graph connected via primary-foreign key relationships and other schema-defined links (Fey et al., 2024). Recent work on task-aware graph construction emphasizes that this lifting step is not neutral: the particular choice of graph representation can fundamentally determine which dependencies are exposed to the learner and which are

⁵Not all tabular foundation models aim to introduce cross-row structure; for instance, CARTE (Kim et al., 2024) represents each row independently and focuses on transfer across heterogeneous tables, and TARTE (Kim et al., 2025) similarly produces row-level representations through semantic pre-training on large knowledge bases. This further illustrates that lifting row-locality is not the defining objective of this line of work.

obscured, amplifying or suppressing the effectiveness of GNNs depending on how well the induced structure aligns with the target task (Cucumides & Geerts, 2025). Despite these insights, the choice of graph construction in much of this literature is still treated primarily as a modeling or engineering decision, with emphasis placed on empirical performance rather than on formally characterizing the representational consequences of lifting tables to graphs. In contrast, we do not propose new graph learning methods or graph constructions; instead, we provide a formalization of the graph-to-table process and introduce a framework and vocabulary for studying expressiveness, clarifying how different graph constructions delimit the class of tabular prediction functions that can be represented.

Tabular models on graph-structured benchmarks. Recent work has shown that strong tabular learners can be competitive on graph benchmarks when augmented with explicit feature constructions that expose local relational or neighborhood information, such as fixed aggregations or structural summaries (Bazhenov et al., 2025; Anonymous, 2025). These results suggest that much of the empirical gap between tabular and graph-based models can be attributed to access to inter-node or inter-row information—often shallow—rather than to architectural differences alone, with tabular models benefiting from their robustness, stable optimization, and ability to handle heterogeneous features once such information is made explicit.

This perspective is related to our case study, but differs from our work in both object and objective. Prior approaches based on neighbor feature aggregation or fixed aggregation features are developed for graph datasets and are primarily used as diagnostic tools for graph benchmarks, where tabular learners serve as “must-beat” baselines (Robinson et al., 2024; Bazhenov et al., 2025): when they match or outperform graph neural networks, the conclusion is that the benchmark does not structurally require learned message passing. By contrast, our focus is on tabular datasets, where relational structure is implicit rather than given. Instead of using tabular models to evaluate the adequacy of graph benchmarks, we study the structural limitations of row-local tabular learning itself, and show that explicitly exposing inter-row structure can complement strong tabular representations even in purely tabular settings.

B. Background

We denote *multisets* by $\{\{\cdot\}\}$ and, for a set X , we write $\text{mset}(X)$ for the collection of all finite multisets over X .

MPNNs and their induced node predictors Fix an input graph $G = (V, E_1, \dots, E_m, \rho)$. A k -layer (*heterogenous*) MPNN (Gilmer et al., 2017; Schlichtkrull et al., 2018) maintains embeddings $\mathbf{h}_v^{(\ell)} \in \mathbb{R}^d$ for each node v and each layer $\ell \in \{0, 1, \dots, k\}$. Initialization is given by a learnable encoder $\mathbf{h}_v^{(0)} = \text{INI}(\rho(v), C(v))$. For each layer $\ell = 0, \dots, k-1$ and edge type $i \in [m]$, it computes

$$\begin{aligned} \mathbf{m}_{v,i}^{(\ell)} &= \text{AGG}_i^{(\ell)} \left(\{\{\text{MSG}_i^{(\ell)}(\mathbf{h}_v^{(\ell)}, \mathbf{h}_u^{(\ell)}) \mid u \in N_i(v)\}\} \right), \\ \mathbf{h}_v^{(\ell+1)} &= \text{UPD}^{(\ell)} \left(\mathbf{h}_v^{(\ell)}, \mathbf{m}_{v,1}^{(\ell)}, \dots, \mathbf{m}_{v,m}^{(\ell)} \right), \end{aligned}$$

where each $\text{MSG}_i^{(\ell)}$ and $\text{UPD}^{(\ell)}$ is a differentiable learnable map and each $\text{AGG}_i^{(\ell)} : \text{mset}(\mathbb{R}^{d'}) \rightarrow \mathbb{R}^{d'}$ is permutation-invariant.

A k -layer MPNN induced a (total) *node classifier* $\text{npred}^{\text{MPNN}}$ by thresholding the final readout embedding:

$$\text{npred}_G^{\text{MPNN}} : V \rightarrow \{0, 1\} : v \mapsto \mathbb{I} \left[\text{READ} \left(\mathbf{h}_v^{(k)} \right) > 0 \right],$$

where $\mathbb{I}[\cdot] \in \{0, 1\}$ is the indicator function and $\text{READ} : \mathbb{R}^d \rightarrow \mathbb{R}$ is a differentiable and learnable *readout* function.

First-order logic We here define standard first-order logic over the *graphs* $G = (V, E_1, \dots, E_m, \rho)$ from the preliminaries.

► *Signature.* We recall that for a given graph $G = (V, E_1, \dots, E_m, \rho)$, we use the binary relation symbols E_1, \dots, E_m to form the *edge signature* $\sigma_G = \{E_1, \dots, E_m\}$. To access node features in logic, we fix a *finite* set \mathcal{U}_ρ of unary predicate symbols. Each $U \in \mathcal{U}_\rho$ is intended to represent a Boolean test on the node annotation $(C(v), \rho(v))$ (e.g., a node-type indicator such as $C(v) = C_0$, or a threshold/equality test on a designated attribute when present). We work over the expanded signature $\sigma_G^\rho = \sigma_G \cup \mathcal{U}_\rho$.

For each graph G , every $U \in \mathcal{U}_\rho$ is interpreted as a set $U^G \subseteq V$. Concretely, one may view \mathcal{U}_ρ as fixing a finite family of

Boolean functions $U : \{(C, \eta) \mid C \subseteq \mathcal{A} \text{ finite}, \eta \in \text{val}^C\} \rightarrow \{0, 1\}$ and set

$$U^G = \{v \in V \mid U(C(v), \rho(v)) = 1\}.$$

► *FO syntax.* Let Var be a countable set of variables. First-order formulas over σ_G^ρ are generated by

$$\varphi := (x = y) \mid U(x) \mid E_i(x, y) \mid \neg\varphi \mid (\varphi \wedge \psi) \mid \exists x \varphi,$$

where $x, y \in \text{Var}$, $U \in \mathcal{U}_\rho$, and $i \in [m]$. We use the usual abbreviations for $\vee, \rightarrow, \forall$.

► *Free variables.* The set $\text{fv}(\varphi) \subseteq \text{Var}$ of *free variables* of an FO formula φ over σ_G^ρ is defined inductively by

$$\begin{aligned} \text{fv}(x = y) &= \{x, y\}, \\ \text{fv}(U(x)) &= \{x\}, \\ \text{fv}(E_i(x, y)) &= \{x, y\}, \\ \text{fv}(\neg\varphi) &= \text{fv}(\varphi), \\ \text{fv}(\varphi \wedge \psi) &= \text{fv}(\varphi) \cup \text{fv}(\psi), \\ \text{fv}(\exists x \varphi) &= \text{fv}(\varphi) \setminus \{x\}. \end{aligned}$$

A formula φ is (*FO*-)*unary* if $\text{fv}(\varphi) \subseteq \{x\}$ for some variable x ; in this case we often write $\varphi(x)$.

► *FO semantics.* A *variable assignment* is a map $\alpha : \text{Var} \rightarrow V$. Satisfaction $G, \alpha \models \varphi$ is defined inductively:

$$\begin{aligned} G, \alpha \models (x = y) &\iff \alpha(x) = \alpha(y), \\ G, \alpha \models U(x) &\iff \alpha(x) \in U^G, \\ G, \alpha \models E_i(x, y) &\iff (\alpha(x), \alpha(y)) \in E_i, \\ G, \alpha \models \neg\varphi &\iff \text{not}(G, \alpha \models \varphi), \\ G, \alpha \models (\varphi \wedge \psi) &\iff (G, \alpha \models \varphi) \text{ and } (G, \alpha \models \psi), \\ G, \alpha \models \exists x \varphi &\iff \exists v \in V : G, \alpha[x \mapsto v] \models \varphi, \end{aligned}$$

where $\alpha[x \mapsto v]$ is α updated to map x to v . If $\varphi(x)$ has exactly one free variable x , we write $G \models \varphi(v)$ to mean $G, \alpha \models \varphi$ for any (equivalently, every) assignment α with $\alpha(x) = v$.

Graded modal logic We also introduce the graded modal logic (GML) fragment of FO.

► *Counting quantifiers.* For $N \in \mathbb{N}$, we write $\exists^{\geq N} y \theta(y)$ as an abbreviation for the FO formula expressing that at least N *distinct* witnesses satisfy θ :

$$\exists y_1 \cdots \exists y_N \left(\bigwedge_{p \neq q} y_p \neq y_q \wedge \bigwedge_{p=1}^N \theta(y_p) \right).$$

Equivalently, for any assignment α , $G, \alpha \models \exists^{\geq N} y \theta(y)$ if and only if

$$|\{v \in V \mid G, \alpha[y \mapsto v] \models \theta(y)\}| \geq N.$$

► *GML syntax and semantics.* The *graded modal logic* (GML) fragment over σ_G^ρ consists of unary formulas $\varphi(x)$ generated by $\varphi(x) :=$

$$U(x) \mid \neg\varphi(x) \mid (\varphi(x) \wedge \psi(x)) \mid \exists^{\geq N} y (E_i(x, y) \wedge \varphi(y)),$$

where $U \in \mathcal{U}_\rho$, $i \in [m]$, and $N \in \mathbb{N}$. Clearly, GML formulas inherit the semantics of FO formulas and the counting quantifiers given earlier.

► *Modal depth.* The modal depth $\text{md}(\varphi)$ of a GML formula is defined by $\text{md}(U(x)) = 0$, $\text{md}(\neg\varphi) = \text{md}(\varphi)$, $\text{md}(\varphi \wedge \psi) = \max\{\text{md}(\varphi), \text{md}(\psi)\}$, and

$$\text{md}(\exists^{\geq N} y (E_i(x, y) \wedge \varphi(y))) = 1 + \text{md}(\varphi).$$

We write $\text{GML}^{(\leq k)}$ for the set of GML formulas of modal depth at most k .

C. Model-induced grables for CARTE, TARTE, TabPFN, and NFA

Here we instantiate graph constructors for three prominent tabular learning methods by making their *tokenization* and *connectivity* explicit as a grable. We also formulate Neighbourhood Feature Augmentation as a grable.

Throughout, let $C = \{c_1, \dots, c_m\}$ be a schema and $T \subseteq \text{val}^C$ a C -table. We use ρ for node features, and we allow edge features/labels (e.g. column-name embeddings) as part of the graph representation.

C.1. CARTE

CARTE (Kim et al., 2024) represents each row as a small multi-relational *graphlet*: a star-shaped graph with a central row token and one leaf per non-missing cell. We formalize this as a constructor that produces a single grable for the whole table by taking the disjoint union of row graphlets.

Example C.1 (CARTE grable). Let $C = \{c_1, \dots, c_m\}$ and T be a C -table. The *CARTE grable* of (C, T) is the graph

$$G_{C,T}^{\text{CARTE}} = (V, E_1, \dots, E_m, \rho, \eta)$$

defined as follows. We allow also for an edge feature map η here. For each row $r \in T$, let $I(r) = \{i \in [m] \mid r[c_i] \neq \text{NaN}\}$ and create a *row center* node v_r and one *cell* node $c_{r,i}$ for each $i \in I(r)$. Thus

$$V = \{v_r : r \in T\} \cup \{c_{r,i} : r \in T, i \in I(r)\}.$$

For each $i \in [m]$, the i -th edge relation is

$$E_i = \{(v_r, c_{r,i}) : r \in T, i \in I(r)\} \quad (\text{optionally also } (c_{r,i}, v_r)).$$

Node features encode values (optionally conditioned on the column):

$$\rho(c_{r,i}) = \phi(c_i, r[c_i]), \quad \rho(v_r) = r,$$

for any fixed featurizer ϕ . Edge features carry column semantics via

$$\eta((v_r, c_{r,i})) = \text{LM}(c_i),$$

for some language model embedding LM. We write γ_{CARTE} for the corresponding constructor. ◀

C.2. TARTE

TARTE (Kim et al., 2025) is a transformer-style tabular backbone that forms representations from *column–cell pairs*: each entry is interpreted in the context of its column name, and the model aggregates information across a row via attention to produce row-level predictions.

Example C.2 (TARTE grable). Let $C = \{c_1, \dots, c_m\}$ and T be a C -table. The *TARTE grable* of (C, T) is the graph

$$G_{C,T}^{\text{TARTE}} = (V, E_{\text{attn}}, E_{\text{row}}, \rho)$$

defined as follows. The node set consists of row nodes and column–cell token nodes:

$$V = \{v_r : r \in T\} \cup \{t_{r,i} : r \in T, i \in [m]\}.$$

Token features encode the column name together with the cell value,

$$\rho(t_{r,i}) = \phi(c_i, r[c_i]), \quad \rho(v_r) = r,$$

for some fixed featurizer ϕ . Edges encode (permissible) attention within each row:

$$E_{\text{attn}} = \{(t_{r,i}, t_{r,j}) : r \in T, i, j \in [m]\}.$$

We also connect each row node to its tokens via

$$E_{\text{row}} = \{(v_r, t_{r,i}) \mid r \in T, i \in [m]\} \quad (\text{optionally also } (t_{r,i}, v_r)).$$

We write γ_{TARTE} for the corresponding constructor. ◀

C.3. TabPFN

TabPFN (Hollmann et al., 2025) consumes an entire table as a single set of tokens. A useful graph-level view is that each transformer block restricts self-attention to either (i) tokens within the same *row* (feature interactions) or (ii) tokens within the same *column* (cross-row information exchange for a fixed feature). Thus, TabPFN can be seen as message passing on a graph whose edges encode permissible attention neighborhoods, together with an alternation schedule over edge types across layers.

Example C.3 (TabPFN grable). Let $C = \{c_1, \dots, c_m\}$ and T be a C -table. The *TabPFN grable* of (C, T) is the graph

$$G_{C,T}^{\text{TabPFN}} = (V, E^{\text{row}}, E^{\text{col}}, \rho),$$

with $V = V_{\text{cell}} \cup V_{\text{row}}$, where

$$V_{\text{cell}} = \{c_{r,i} \mid r \in T, i \in [m]\}, \quad V_{\text{row}} = \{v_r \mid r \in T\}.$$

Row- and column-wise attention relations are

$$\begin{aligned} E^{\text{row}} &= \{(c_{r,i}, c_{r,j}) \mid r \in T, i, j \in [m]\} \cup \\ &\quad \{(v_r, c_{r,i}), (c_{r,i}, v_r) \mid r \in T, i \in [m]\}, \\ E^{\text{col}} &= \{(c_{r,i}, c_{s,i}) \mid r, s \in T, i \in [m]\}. \end{aligned}$$

Node features are initialized by

$$\rho(c_{r,i}) = \psi(c_i, r[c_i]), \quad \rho(v_r) = r,$$

for some featurizer ψ . We write γ_{TabPFN} for the corresponding constructor. \blacktriangleleft

C.4. NFA

Neighborhood Feature Aggregation (NFA) (Bazhenov et al., 2025) is a *derived* constructor: it requires a starting grable $G_{C,T}^{\gamma}$ to define 1-hop neighborhoods, but its output is a *trivial grable* so that downstream learners can be purely tabular.

Example C.4 (NFA grable (trivial output)). Fix a base constructor γ and let

$$G_{C,T}^{\gamma} = (V, E_1, \dots, E_m, \rho)$$

be its grable on (C, T) with row nodes $V_{\text{row}} = \{v_r \mid r \in T\}$. Write $E = \bigcup_{i=1}^m E_i$ and $N(v) = \{u \in V_{\text{row}} \mid (v, u) \in E\}$ (row-node neighbors).

Define the NFA augmentation for a row node $v \in V_{\text{row}}$ as follows. For any scalar feature coordinate z (numerical, or a one-hot indicator derived from a categorical feature), let

$$S_z(v) = \{z(u) \mid u \in N(v), z(u) \neq \text{NaN}\}.$$

Then $\text{NFA}(v)$ concatenates: (i) for each numerical coordinate z : $\text{mean}(S_z(v)) \parallel \text{min}(S_z(v)) \parallel \text{max}(S_z(v))$; (ii) for each one-hot indicator z of each categorical feature: $\text{mean}(S_z(v))$.

Set the enriched row features to

$$\rho^{\text{NFA}}(v) = \rho(v) \parallel \text{NFA}(v) \quad (v \in V_{\text{row}}).$$

Finally, the *NFA grable* is the *trivial grable* on row nodes with these features:

$$G_{C,T}^{\text{NFA}} = (V_{\text{row}}, \emptyset, \rho^{\text{NFA}}).$$

We write $\gamma_{\text{NFA}}(\gamma)$ for the resulting constructor. \blacktriangleleft

D. Grabular expressiveness

D.1. Proof of Proposition 3.1

Fix $k \in \mathbb{N}$. We need to show that for any k -layer MPNN node classifier on $G_{C,T}^{\text{triv}}$, there exists a function $F : \text{val}^C \rightarrow \{0, 1\}$ (determined by the learned parameters) such that for all $r \in T$,

$$\text{npred}_{G_{C,T}^{\text{triv}}}^{\text{MPNN}}(v_r) = F(r).$$

Indeed, by definition of the trivial constructor, $G_{C,T}^{\text{triv}}$ has no edges of any type, so for every row node v_r and every layer ℓ the neighbour multiset used by the aggregator is empty. Hence the aggregated message at layer ℓ is the same constant for all nodes:

$$\mathbf{m}^{(\ell)}(v_r) = \text{Agg}^{(\ell)}(\emptyset) =: \mathbf{c}_\ell,$$

which does not depend on T or on r . We can now write the embeddings computed by the MPNN as

$$\mathbf{h}_{v_r}^{(0)} = g(r), \quad \mathbf{h}_{v_r}^{(\ell+1)} = \text{Upd}^{(\ell)}(\mathbf{h}_{v_r}^{(\ell)}, \mathbf{m}^{(\ell)}(v_r)) \quad (\ell = 0, \dots, k-1),$$

and final prediction

$$\text{npred}_{G_{C,T}^{\text{triv}}}^{\text{MPNN}}(v_r) = \text{Read}(\mathbf{h}_{v_r}^{(k)}).$$

Substituting $\mathbf{m}^{(\ell)}(v_r) = \mathbf{c}_\ell$ yields

$$\mathbf{h}_{v_r}^{(\ell+1)} = \text{Upd}^{(\ell)}(\mathbf{h}_{v_r}^{(\ell)}, \mathbf{c}_\ell),$$

so the evolution of $\mathbf{h}_{v_r}^{(\ell)}$ depends only on the initial feature $g(r)$.

Define functions $g_\ell : \text{val}^C \rightarrow \mathbb{R}^d$ recursively by

$$g_0(r) := g(r), \quad g_{\ell+1}(r) := \text{Upd}^{(\ell)}(g_\ell(r), \mathbf{c}_\ell).$$

Then by induction on ℓ we have $\mathbf{h}_{v_r}^{(\ell)} = g_\ell(r)$ for all $\ell \leq k$, and in particular $\mathbf{h}_{v_r}^{(k)} = g_k(r)$. Now define the row-wise classifier

$$F : \text{val}^C \rightarrow \{0, 1\}, \quad F(r) := \text{Read}(g_k(r)).$$

Therefore, for every $r \in T$,

$$\text{npred}_{G_{C,T}^{\text{triv}}}^{\text{MPNN}}(v_r) = \text{Read}(\mathbf{h}_{v_r}^{(k)}) = \text{Read}(g_k(r)) = F(r),$$

as claimed.

D.2. Proof of Proposition 3.3

We need to show that each predictor in Figure 1 is not row-local. We exhibit, for each task, an instance where the label of a fixed row r changes after adding rows (while keeping r itself unchanged), hence the predictor is not row-local.

UNIQUE. Let $T = \{r\}$ where $r[a_i] = v$ for some column a_i . Then v appears only in r , so $\text{UNIQUE}(r) = 1$. Let $T' := \{r, s\}$ where $s[a_i] = v$ and s agrees with r on a_i (other columns arbitrary). Then v is no longer unique to r , so $\text{UNIQUE}(r) = 0$ in T' .

COUNT_N. Let $T = \{r\}$, so there are 0 other rows sharing any value with r , hence $\text{COUNT}_N(r) = 0$. Add N fresh rows s_1, \dots, s_N with $s_j[a_i] = r[a_i]$ for the designated column a_i (others arbitrary). In the enlarged table T' we have at least N other rows sharing that value with r , hence $\text{COUNT}_N(r) = 1$.

DOUBLE. Pick $T = \{r\}$ so no witness row exists and $\text{DOUBLE}(r) = 0$. Add a row s that shares the designated value with r and satisfies the required local constraint (unary predicate on s 's own features). Then $\text{DOUBLE}(r) = 1$ in $T' := \{r, s\}$.

DIAMOND. Pick $T = \{r\}$ so no other row exists and $\text{DIAMOND}(r) = 0$. Add a row s such that $s[a_i] = r[a_i]$ and $s[a_j] = r[a_j]$ for two designated columns $a_i \neq a_j$. Then s witnesses the required double-overlap and $\text{DIAMOND}(r) = 1$ in $T' := \{r, s\}$.

In all four cases, $\text{rpred}_{C,T}(r) \neq \text{rpred}_{C,T'}(r)$ for some $T \subseteq T'$, so none of these predictors is row-local. Equivalently, none lies in $\text{Expr}(\{\gamma_{\text{triv}}\}, \mathcal{P})$ for any \mathcal{P} .

D.3. Proof of Proposition 3.4

Let $\mathcal{P}_{\text{MPNN}}^{(k)}$ denote k -layer MPNNs. We need to show that

- **UNIQUE, COUNT_N** $\in \text{Expr}(\{\gamma_{\text{inc}}\}, \mathcal{P}_{\text{MPNN}}^{(2)})$,
- **DOUBLE** $\in \text{Expr}(\{\gamma_{\text{inc}}\}, \mathcal{P}_{\text{MPNN}}^{(3)})$.

We write the three targets as GML formulas using the counting modality $\exists^{\geq N} y (E_i(x, y) \wedge \varphi(y))$ from the grammar. Let $\text{Row}(\cdot)$ and $\text{Val}(\cdot)$ be unary predicates distinguishing row and value nodes in γ_{inc} (and let $P(\cdot) \in \mathcal{U}_\rho$ be the unary “local condition” used in DOUBLE).

UNIQUE. Fix the intended meaning: r has some column–value neighbor that is incident to no other row. For each column type i , define

$$\psi_{\text{uniq},i}(x) := \exists^{\geq 1} y (E_i(x, y) \wedge \text{Val}(y) \wedge \neg \exists^{\geq 2} z (E_i(y, z) \wedge \text{Row}(z))),$$

and let $\psi_{\text{uniq}}(x) := \bigvee_i \psi_{\text{uniq},i}(x)$. At a row node $x = v_r$, the inner negated counting condition says that the chosen value node $y = u_{i,v}$ has fewer than two adjacent row nodes via E_i , i.e. it is adjacent to exactly one row (namely v_r). Thus ψ_{uniq} defines UNIQUE. Its modal depth is 2.

COUNT_N. Assume the designated column type is i (otherwise disjoin over the permitted choices). Define

$$\psi_{\text{cnt},N}(x) := \exists^{\geq 1} y (E_i(x, y) \wedge \text{Val}(y) \wedge \exists^{\geq (N+1)} z (E_i(y, z) \wedge \text{Row}(z))).$$

At $x = v_r$, this picks a value node $y = u_{i,v}$ adjacent to r whose E_i -row-neighborhood has size at least $N + 1$, i.e. at least N other rows share that value with r . This has modal depth 2.

DOUBLE. Assume the task is witnessed by a length-3 pattern $v_r - u_{i,v} - v_s - u_{j,w}$ where v_s satisfies the unary predicate P . Define

$$\psi_{\text{dbl}}(x) := \exists^{\geq 1} y (E_i(x, y) \wedge \text{Val}(y) \wedge \exists^{\geq 1} s (E_i(y, s) \wedge \text{Row}(s) \wedge P(s) \wedge \exists^{\geq 1} w (E_j(s, w) \wedge \text{Val}(w)))).$$

Starting from a row node $x = v_r$, this moves to an i -value node y , then to an i -adjacent row s satisfying P , and finally to a j -value node w , exactly as required. This has modal depth 3.

Hence UNIQUE and COUNT_N are definable in GML^(≤2) and DOUBLE in GML^(≤3) on γ_{inc} . By Theorem 1.1, these properties are realized by 2-layer (resp. 3-layer) MPNNs, giving the claimed membership in $\text{Expr}(\{\gamma_{\text{inc}}\}, \mathcal{P}_{\text{MPNN}}^{(k)})$.

D.4. Proof of Proposition 3.5

We need to show that for every $k \in \mathbb{N}$,

$$\text{DIAMOND} \notin \text{Expr}(\{\gamma_{\text{inc}}\}, \mathcal{P}_{\text{MPNN}}^{(k)}).$$

Proof sketch. Fix $k \in \mathbb{N}$. We construct two tables T and T' over a schema containing two designated columns $c_i \neq c_j$ (and, if needed, additional fresh columns to realize fillers). Let r be the distinguished row in both tables, with $r[c_i] = \alpha$ and $r[c_j] = \beta$.

In table T , include, besides r , a single row s with $s[c_i] = \alpha$ and $s[c_j] = \beta$. Then in the incidence graph $G = G_{C,T}^{\gamma_{\text{inc}}}$, the row node v_r has a diamond witness v_s via the value nodes $u_{i,\alpha}$ and $u_{j,\beta}$, so $\text{DIAMOND}(r) = 1$.

In table T' , replace s by two rows s_i, s_j where $s_i[c_i] = \alpha$ but $s_i[c_j] \neq \beta$, and $s_j[c_j] = \beta$ but $s_j[c_i] \neq \alpha$ (choose fresh values for the other entries). Then in $H := G_{C,T'}^{\gamma_{\text{inc}}}$ there is no single row that overlaps with r on both c_i and c_j , so $\text{DIAMOND}(r) = 0$.

We now make G and H k -GML-indistinguishable. More specifically, we add the same multiset of *filler* rows to both tables so that every value node that occurs within distance $\leq k$ from v_r has the same number of incident row neighbors of each unary feature-type in G and in H . Concretely, for each value node whose degree differs between the two constructions (initially $u_{i,\alpha}$ and $u_{j,\beta}$), add enough fresh rows using fresh values in other columns so as to equalize all relevant degrees and local unary predicates. This equalization can be done independently for each such value node because incidence graphs are bipartite and edges are typed by columns.

After this padding, the pointed incidence graphs (G, v_r) and (H, v_r) are k -round counting-bisimilar, and therefore satisfy the same GML^(≤k) formulas.

The two tables yield incidence graphs indistinguishable by GML^(≤k) at v_r , yet they disagree on DIAMOND. Hence DIAMOND is not definable in GML^(≤k) for any k . Since DIAMOND is FO-definable on γ_{inc} but not in GML^(≤k), Theorem 1.1 implies that no k -layer MPNN realizes DIAMOND on γ_{inc} . \square

D.5. Extended incidence graph

We show that, by using an extended incidence constructor we can express DIAMOND using MPNNs. Indeed, fix two designated columns $c_i \neq c_j$. Define an extended constructor $\gamma_{\text{inc}}^{(2)}$ as follows. Starting from the incidence grable $G_{C,T}^{\gamma_{\text{inc}}}$, add a new node $p_{\alpha,\beta}$ for every pair (α, β) that occurs in columns (c_i, c_j) of some row in T , and add a new edge type E_{ij} such that

$$(v_r, p_{\alpha,\beta}) \in E_{ij} \iff r[a_i] = \alpha \wedge r[a_j] = \beta.$$

Let $\text{Pair}(\cdot) \in \mathcal{U}_\rho$ be a unary predicate true exactly on these pair nodes, and this predicate is now available for the logic GML.

On $G_{C,T}^{\gamma_{\text{inc}}^{(2)}}$, the task DIAMOND is defined by the GML formula

$$\psi_{\diamond}(x) := \exists^{\geq 1} p \left(E_{ij}(x, p) \wedge \text{Pair}(p) \wedge \exists^{\geq 2} y (E_{ij}(p, y) \wedge \text{Row}(y)) \right).$$

Indeed, for a row node $x = v_r$, the outer quantifier selects the pair node $p_{r[a_i], r[a_j]}$ representing the joint value $(r[a_i], r[a_j])$. The inner counting condition requires that this pair node be incident (via E_{ij}) to at least two row nodes, namely v_r and some other v_s , which is equivalent to the existence of a single other row $s \neq r$ sharing *both* values with r .

Thus $\psi_{\diamond} \in \text{GML}^{(\leq 2)}$, and by Theorem 1.1 it follows that

$$\text{DIAMOND} \in \text{Expr}(\{\gamma_{\text{inc}}^{(2)}\}, \mathcal{P}_{\text{MPNN}}^{(2)}).$$

This is again a nice illustration of the constructor/grable formalism: a minimal change to the constructor (turning a two-hop conjunction into a single edge type) immediately collapses an FO-only pattern into shallow GML, and hence into constant-depth message passing.

E. Time-Aware NFA

We describe a *time-aware* variant of Neighbourhood Feature Aggregation (NFA), which is a specialization of the construction introduced in Appendix C.4. The purpose of this variant is to enforce temporal causality in transactional and sequential settings, while preserving the representation format and notation of NFA.

Example E.1 (Time-aware NFA grable). Fix a base constructor γ and let

$$G_{C,T}^{\gamma} = (V, E_1, \dots, E_m, \rho)$$

be its grable on (C, T) with row nodes $V_{\text{row}} = \{v_r \mid r \in T\}$, as in Appendix C.4. Assume that each row $r \in T$ is associated with a timestamp $t(r) \in \mathbb{R}$, stored as one of the row attributes.

Write $E = \bigcup_{i=1}^m E_i$ and $N(v) = \{u \in V_{\text{row}} \mid (v, u) \in E\}$. For a fixed time window $W > 0$, define the *time-aware neighborhood* of a row node $v \in V_{\text{row}}$ as

$$N_W(v) = \{u \in N(v) \mid t(u) < t(v) \wedge t(v) - t(u) \leq W\}.$$

The time-aware NFA augmentation for a row node $v \in V_{\text{row}}$ is defined exactly as in Appendix C.4, except that all aggregations are computed over $N_W(v)$ instead of $N(v)$. Specifically, for any scalar feature coordinate z (numerical, or a one-hot indicator derived from a categorical feature), let

$$S_z^{(W)}(v) = \{z(u) \mid u \in N_W(v), z(u) \neq \text{NaN}\}.$$

Then $\text{NFA}_W(v)$ concatenates: (i) for each numerical coordinate z : $\text{mean}(S_z^{(W)}(v)) \parallel \text{min}(S_z^{(W)}(v)) \parallel \text{max}(S_z^{(W)}(v))$; (ii) for each one-hot indicator z of each categorical feature: $\text{mean}(S_z^{(W)}(v))$.

The enriched row features are given by

$$\rho^{\text{NFA}(W)}(v) = \rho(v) \parallel \text{NFA}_W(v) \quad (v \in V_{\text{row}}).$$

Finally, the *time-aware NFA grable* is the *trivial* grable on row nodes with these features:

$$G_{C,T}^{\text{NFA}(W)} = (V_{\text{row}}, \emptyset, \rho^{\text{NFA}(W)}).$$

We write $\gamma_{\text{NFA}(W)}(\gamma)$ for the resulting constructor. ◀

Discussion. This construction does not introduce a new representation class. It is a time-restricted instance of NFA, obtained by replacing the neighborhood $N(v)$ in Appendix C.4 with its temporally filtered variant $N_W(v)$. All expressiveness considerations for NFA therefore apply unchanged.

F. Experimental setup

F.1. Datasets

F.1.1. SYNTHETIC TRANSACTIONS DATASET

We construct a synthetic transaction dataset to study learning scenarios in which prediction targets depend on relationships between rows, while keeping the data representation itself purely tabular. Each row corresponds to a single transaction and contains only standard tabular attributes; no explicit relational or graph structure is encoded in the dataset.

Tabular schema. Each transaction is represented by the following columns:

- `id`: a unique, sequential transaction identifier.
- `card_id`: a categorical identifier representing the payment card used.
- `merchant_id`: a categorical identifier representing the merchant.
- `merchant_city`: a categorical attribute indicating the merchant’s city, or the special value `ONLINE` for online merchants.

Merchant generation. A fixed pool of merchants is generated for each dataset split. Each merchant is assigned a unique integer identifier. Merchants are independently labeled as *online* with a fixed probability (the *online share*); online merchants are assigned the city label `ONLINE`. All remaining merchants are considered physical and are assigned a city sampled uniformly at random from a predefined list of European cities. The merchant city attribute is therefore a deterministic function of the merchant identifier.

Card generation and coverage. Card identifiers are generated as formatted strings (e.g., `C000317`) to mimic realistic identifiers and avoid numerical formatting issues. To prevent degenerate cases where a card never appears, the data generation process enforces that *every card identifier occurs at least once*. This is achieved by assigning each card to exactly one transaction before any additional sampling takes place.

Transaction-level sampling. After guaranteeing one occurrence per card, the remaining transactions are populated by sampling card identifiers with replacement from the card pool. Sampling probabilities follow a bounded power-law distribution, so that some cards appear more frequently than others. This induces heterogeneous card usage frequencies while maintaining full coverage.

Merchant identifiers are sampled independently for each transaction, also using a skewed distribution. As a result, a small number of merchants account for a disproportionate number of transactions, while most merchants appear infrequently. This design reflects common properties of real transaction data and is critical for inducing non-trivial inter-row dependencies.

Assembly and randomization. Transaction rows are assembled by combining transaction identifiers, sampled card identifiers, and sampled merchant identifiers, and then joining with the merchant table to attach the corresponding city attribute. The resulting table is randomly shuffled to remove any ordering artifacts introduced by the card-coverage step. After shuffling, transaction identifiers are reassigned to ensure they remain sequential.

Train, validation, and test splits. Training, validation, and test datasets are generated independently using the same procedure but with different random seeds and dataset sizes. No identifiers are shared across splits, ensuring an inductive evaluation setting. The exact dataset sizes and parameters are summarized in Table 4.

Example rows. Table 3 shows representative rows from a generated dataset. Card and merchant identifiers repeat across rows, and the merchant city attribute is entirely determined by the merchant identifier.

Table 3. Example rows from the synthetic transaction dataset.

id	card_id	merchant_id	merchant_city
1	C000317	42	Brussels
2	C000102	17	ONLINE
3	C000317	105	Paris
4	C000891	42	Brussels
5	C000045	311	Berlin
6	C000102	17	ONLINE

Dataset statistics. Table 4 reports summary statistics for each split. By construction, every card appears at least once in each split, while both card usage and merchant usage exhibit heavy-tailed frequency distributions.

Table 4. Summary statistics of the synthetic transaction datasets.

Statistic	Train	Validation	Test
# transactions	8,000	1,000	1,000
# unique cards	2,500	350	350
# unique merchants	3,500	300	300
Online merchants	0.15	0.12	0.12

This generation process deliberately separates *representation* from *structure*: although the data are provided as a simple table, repeated categorical values induce implicit cross-row dependencies. This allows us to precisely control which prediction tasks require reasoning beyond independent rows, while avoiding confounds introduced by explicit relational encodings.

F.1.2. REAL TRANSACTIONS DATASET (RETAIL)

We use a transactional dataset containing all purchases recorded between 01/12/2010 and 09/12/2011 for a UK-based, registered non-store online retailer. The dataset consists of 541,909 transaction records with six numerical features and exhibits multivariate, sequential, and time-series characteristics. Each row corresponds to an individual transaction line item associated with a specific invoice, customer, and timestamp. The retailer primarily sells unique, all-occasion gifts, and a substantial fraction of its customers are wholesalers. For our experiments, we restrict attention to the final 10% of the data in chronological order. This subset is further split based on timestamps into training, validation, and test sets using a 90/10/10 temporal split, ensuring strict temporal consistency and preventing information leakage across splits.

Table 5 shows a simplified example of transaction rows from the dataset. Each row represents a single purchased item within an invoice; multiple rows may share the same invoice number, customer identifier, and timestamp.

InvoiceNo	StockCode	Description	Qty	InvoiceDate	Price	CustomerID	Country
581220	16225	Rattle Snake Eggs	24	2011-12-08 09:39	0.39	13924	UK
581220	16258A	Swirly Circular Rubbers (Bag)	36	2011-12-08 09:39	0.19	13924	UK
581220	21411	Gingham Heart Doorstop (Red)	8	2011-12-08 09:39	1.95	13924	UK

Table 5. Illustrative example of transaction rows (synthetic but representative). Multiple rows correspond to distinct items within the same invoice.

F.1.3. RELBENCH-TRIAL

The `relnbench-trial` dataset is a relational clinical trial database derived from the Aggregate Analysis of ClinicalTrials.gov (AACT) initiative, which consolidates protocol and results information for studies registered on ClinicalTrials.gov. The dataset contains structured metadata describing clinical studies, including study design characteristics, interventions, conditions, outcomes, eligibility criteria, sponsors, facilities, and administrative information.

The dataset is organized as a multi-table relational database consisting of 15 tables. The primary table for prediction tasks is `studies`, where each row corresponds to a single registered clinical trial. This table includes high-level descriptive attributes such as study type, phase, enrollment information, allocation, masking, intervention model, sponsor details, and study status. The prediction target is defined at the level of the `studies` table following the RelBench task specification.

The remaining tables provide auxiliary information linked to studies through primary–foreign key relationships. These tables describe clinical conditions, interventions, outcomes, design groups, sponsors, facilities, and eligibility criteria, among others. Together, these tables define a heterogeneous relational schema, which is illustrated in Figure 4.

The temporal coverage of the dataset begins on January 1, 2000. The dataset follows the RelBench benchmark protocol, which defines time-based splits and prediction windows.

Table 6. Summary statistics of the `relbench-trial` dataset.

Attribute	Value
Domain	Medical
Number of tables	15
Number of rows	5,852,157
Number of columns	140
Start date	2000-01-01
Validation timestamp	2020-01-01
Test timestamp	2021-01-01
Prediction time window	1 year

F.2. Logical tasks generation

To evaluate models on controlled inter-row dependencies, we derive binary classification labels from a given transaction table by applying four deterministic labeling functions. Each function maps the input table to an augmented table by adding one new label column. Importantly, all labels are defined *within a single split* (train/validation/test) using only the rows in that split; the label of a row therefore depends on the multiset of values present in the corresponding split, rather than on any external data.

Throughout, let D denote a table with rows indexed by $i \in \{1, \dots, |D|\}$ and columns (attributes) such as `card_id`, `merchant_id`, and `merchant_city`. Each task produces a label $y_i \in \{0, 1\}$ for each row i .

Task 1: UNIQUE Given a column c , the uniqueness task labels a row as positive if its value in column c occurs *exactly once* in the entire table. In the implementation, we compute the frequency (value count) of each distinct value in column c and set the label to 1 precisely for rows whose value has frequency 1.

Task 2: COUNT and COUNT(=). Given a column c and an integer threshold k , the counting task labels a row based on how often its value appears in column c across the table. Two variants are supported:

- **Greater-than variant:** $y_i = 1$ iff the value in column c appears more than k times.
- **Equality variant:** $y_i = 1$ iff the value in column c appears exactly k times.

Operationally, both variants are implemented by computing value counts for column c and mapping the corresponding count back to each row before applying the threshold test.

Task 3: DOUBLE (existence of another matching row with an anchor attribute). Given two columns c_1 and c_2 , and a designated anchor value a in column c_2 , the double-condition task labels a row as positive if there exists *another* row that shares the same c_1 value and whose c_2 value equals the anchor. The implementation computes, for each distinct value v of c_1 , how many rows satisfy $(c_1 = v) \wedge (c_2 = a)$. This count is then mapped back to each row. To enforce the “other row” requirement, the labeling distinguishes two cases:

- If $D[i, c_2] \neq a$, then $y_i = 1$ iff there is at least one anchor row with the same c_1 value.
- If $D[i, c_2] = a$, then $y_i = 1$ iff there are at least two anchor rows with the same c_1 value (so that one of them can serve as the required distinct witness row).

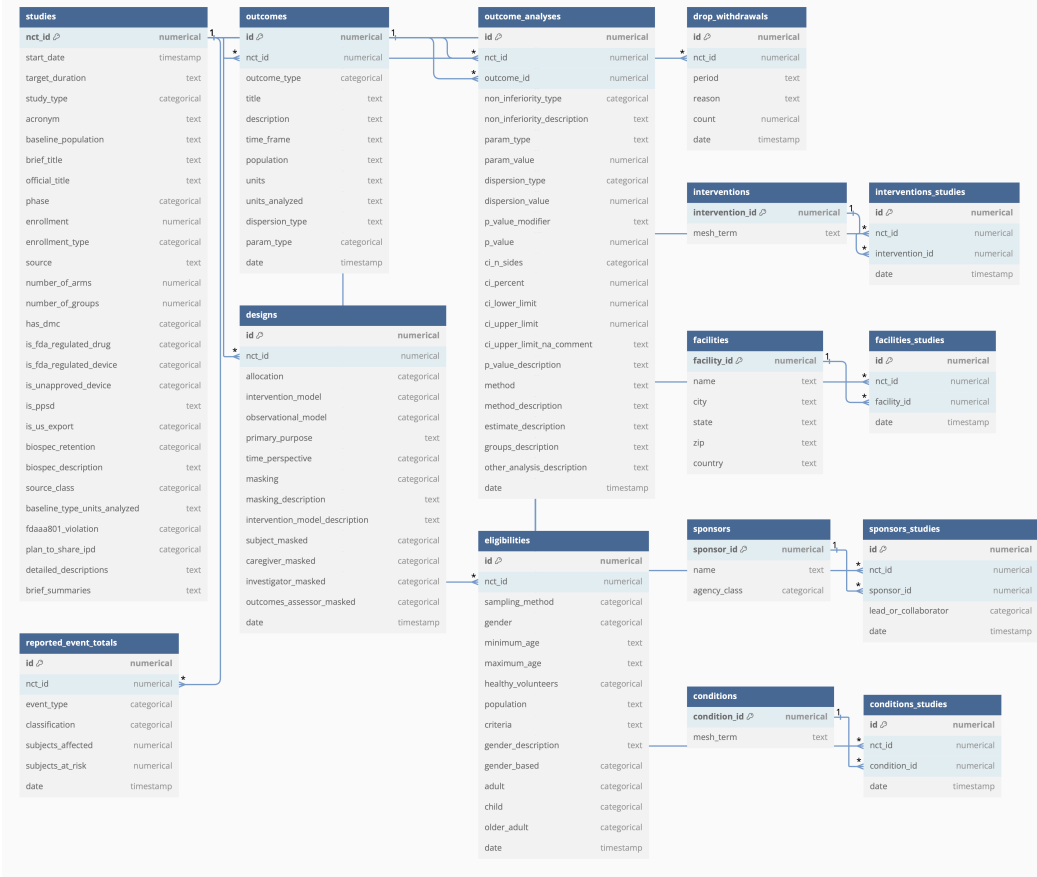


Figure 4. Relational schema of the `relbench-trial` relational dataset. The task studied is associated with table `studies` that contain descriptive information about the clinical studies. Taken from <https://relbench.stanford.edu/datasets/rel-trial/>

Task 4: DIAMOND (duplicate pair). Given two columns c_1 and c_2 , the diamond task (implemented as duplicate-pair detection) labels a row as positive if its (c_1, c_2) pair occurs in more than one row. In the implementation, we group by the pair (c_1, c_2) , compute group sizes, and assign label 1 to all rows belonging to groups of size greater than 1.

Summary. All four labeling functions are deterministic and depend on global frequency or co-occurrence properties of the table. Consequently, labels are *extension-sensitive*: duplicating, removing, or adding rows can change the label of an existing row. This property is central to our experimental objective of isolating tasks that cannot be represented by strictly row-local predictors without access to inter-row information.

Table 7 shows the resulting statistics of the tasks labels in both datasets for the different splits

F.3. Tabular models settings

To fit tabular models LightGBM and RealMLP we use AutoML library Autogluon. Performance report of table 1 correspond to adjusting for 5 minutes in medium quality setting. Relaxing these constraint did not improve performance.

F.4. TabPFN settings and finetuning

We use the last released version of TabPFN which is TabPFN2.5 (Grinsztajn et al., 2025). We evaluate the tasks with and without finetuning. In general, as seen in Table 8 the finetuning effect is not consistent for all tasks and in some cases it degrades model performance.

Table 7. Proportion of presence of label tasks across train, validation, and test splits for each dataset

Dataset	Task	Train (%)	Val (%)	Test (%)
Synthetic Data	UNIQUE	13.1	6.6	7.5
Synthetic Data	COUNT	24.9	18.0	18.4
Synthetic Data	COUNT(=)	15.4	15.0	14.1
Synthetic Data	DOUBLE	48.2	42.8	43.4
Synthetic Data	DIAMOND	30.7	28.1	24.6
Retail Data	UNIQUE	0.9	14.2	10.5
Retail Data	COUNT	47.0	44.6	55.8
Retail Data	COUNT(=)	1.4	2.7	1.3
Retail Data	DOUBLE	41.4	42.0	50.6
Retail Data	DIAMOND	15.5	6.0	4.5

Table 8. Effect of finetuning for TabPFN on logical tasks in the synthetic data.

TASK	METRIC	ORIGINAL	FINETUNED	ABS. DIFF.	REL. GAIN/LOSS
UNIQUE	ROC_AUC	0.8230	0.8744	+0.0514	+6.25%
UNIQUE	F1	0.0250	0.0240	-0.0010	-4.00%
COUNT	ROC_AUC	0.9620	0.9290	-0.0330	-3.43%
COUNT	F1	0.7750	0.8810	+0.1060	+13.68%
COUNT(=)	ROC_AUC	0.3400	0.3310	-0.0090	-2.65%
COUNT(=)	F1	0.0550	0.0137	-0.0413	-75.09%
DOUBLE	ROC_AUC	0.6700	0.8260	+0.1560	+23.28%
DOUBLE	F1	0.6990	0.7550	+0.0560	+8.01%
DIAMOND	ROC_AUC	0.8680	0.8671	-0.0009	-0.10%
DIAMOND	F1	0.7020	0.7258	+0.0238	+3.39%

F.5. Graph learning setting and models.

F.5.1. SYNTHETIC DATA SETUP

Graph construction. For synthetic experiments, we represent the data as a heterogeneous graph composed of a single *transaction* node type (denoted `row`) and multiple *categorical value* node types corresponding to discrete attributes (e.g., card identifiers, merchant identifiers, locations). Each transaction node is connected by a directed edge to exactly one node of each categorical type. Reverse edges are added for all relations, enabling information to propagate back to transaction nodes.

Node initialization. Transaction nodes are initialized with either constant features or a learned type embedding. Categorical value nodes do not carry attributes and are initialized structurally as the sum of: (i) a learnable node-type embedding, and (ii) a fixed, deterministic random hash vector. The fixed hash vectors are non-trainable and serve to break symmetry between nodes with identical initial features and neighborhoods, which is particularly important in inductive settings.

Message passing. We use a multi-layer heterogeneous GraphSAGE architecture. For each relation type, messages are computed using a GraphSAGE convolution with *sum aggregation*, preserving degree and count information. Messages from different relations are summed at each destination node. All message passing is performed in full-batch mode to avoid distortions of node degrees. Each layer applies a ReLU nonlinearity and optional dropout.

Prediction head and training. After the final message-passing layer, transaction node embeddings are passed through a shallow multilayer perceptron to produce a binary logit. Models are trained using a weighted binary cross-entropy loss to account for class imbalance. Decision thresholds are selected on a validation set to maximize the F1 score.

This model serves as a clean structural baseline, designed to evaluate the representational capacity of message-passing GNNs for logical and counting predicates under idealized conditions.

Table 9. Training hyperparameters for synthetic dataset across different tasks.

Hyperparameter	Uniqueness	Count (>)	Count (=)	Double condition	Diamond
Layers	2	2	3	3	4
Hidden dimension	64	64	128	64	64
Dropout	0.0	0.0	0.0	0.0	0.0
Learning rate	1e-3	1e-3	1e-3	1e-3	1e-3
Weight decay	1e-4	1e-4	1e-6	1e-4	1e-4
Aggregation	sum	sum	sum	sum	sum
Epochs	75	75	150	75	75

Training hyperparameters. Table 9 displays the training hyperparameter per tasks.

F.5.2. REAL TRANSACTION DATA SETUP

Graph construction. For real transaction data, we use the same heterogeneous graph schema but including *all* available features (e.g., card, client, merchant, city, state). This setting reflects realistic relational noise, where multiple relations coexist and only a subset may be relevant to a given prediction task. As in the synthetic setting, reverse edges are added for all relations.

Separate graphs are constructed for training, validation, and testing. Node identities are not shared across splits, ensuring an inductive evaluation protocol.

Node initialization. Transaction nodes are initialized from real-valued feature vectors derived from tabular attributes (e.g., transaction amount, time features, and hashed categorical indicators). These features are linearly projected into the hidden embedding space.

Feature-value nodes do not carry attributes and are initialized structurally using the same mechanism as in the synthetic data setting: a learnable type embedding plus a fixed deterministic hash vector. This ensures symmetry breaking without relying on shared node identities across splits.

Message passing and training. Both the model architecture and training hyperparameters are kept constant from the synthetic data case.

F.5.3. CASE STUDY DATA SETUP

For the case study, we distinguish three models.

1. **Tab.** A tree-based row-local (potentially ensemble) method trained using AutoGluon over all of their tree-based method. Best model is chosen using validation ROC-AUC
2. **GNN on tabular incidence graph.** HeteroSage architecture trained on the incidence graph.
3. **GNN on relational entity graph.** To allow fair comparison, we use the GNN proposed by [Robinson et al. \(2024\)](#) with the same training hyperparameters.

The tree-based model can either be fed with the original tabular features (e.g. Tree(T)), or with the original features plus GNN-learned embeddings (which range from 64 to 128 new added dimensions).

G. More experimental results and analysis

G.1. Synthetic data

G.1.1. SENSITIVITY ANALYSIS

To assess the consistency of the models in the logical task, we perform a sensitivity analysis where we perturb the test set (while keeping the distributions parameter constant).

Figure 5 shows the variation of F1-score of models LightGBM, RealMLP and Sage in 5 different perturbations of the test set.

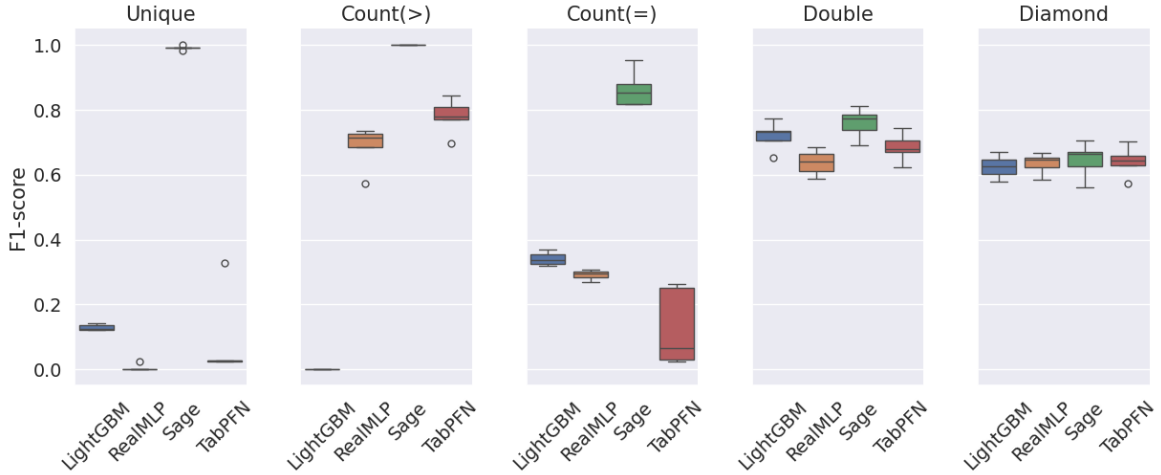


Figure 5. Box-plots for F1 score of models LightGBM, RealMLP, Sage and TabPFN in 5 different perturbations of the original test set.

G.1.2. STRESS-TEST SET

Motivated by the unexpectedly strong performance of tabular models on several tasks, we construct a stress-test set designed to eliminate spurious correlations that could lead to artificially inflated evaluation scores. In particular, this stress-test explicitly removes row-local cues and feature interactions that allow correct predictions without modeling cross-row dependencies.

The construction enforces that successful prediction of the target requires aggregating information across multiple rows. Consequently, any strategy based solely on per-row statistics, local feature patterns, or marginal distributions is insufficient to achieve above-chance performance. This setting therefore provides a controlled evaluation of whether models genuinely capture the intended relational structure of the task, rather than exploiting accidental shortcuts.

Stress test set generation. To create the stress test set, we analyze the possible *row-local shortcuts* that might lead to high performance of tabular datasets in the logical tasks

- **UNIQUE:** No signs of row-local shortcuts. Stress set is generated flipping labels, records with features that were unique in training, are non-unique in stress-test
- **COUNT:** With inequality (higher-than count) most frequent values in training are also more frequent values in validation in test and might serve as proxy. Stress-set generation ensures that high-count value features in train appear below threshold in stress-test. For the equality case, we do not see signs of row-local proxies for the tasks.
- **DOUBLE:** can be approximated by single condition, in particular the most frequent condition of the two. Stress-test ensures that the double condition cannot be well approximated via a single condition (feature = value)
- **DIAMOND:** can be approximated by taking most popular values: stress-set contains a more balanced sample so taking the most popular value of one feature at training does not provide a good proxy for repetition

Results on stress test set. Figure 6 shows the results of models in the stress-test sets for each task.

G.2. Transactional data

G.2.1. REMOVING DISTRACTING INFORMATION.

To address how the extra information coming from the features that are not considered in the logical tasks affect the learning and performance of the different models, we create a simplified version of the dataset, where only features used in the creation of the logical tasks are considered. This mirrors the synthetic dataset properties.

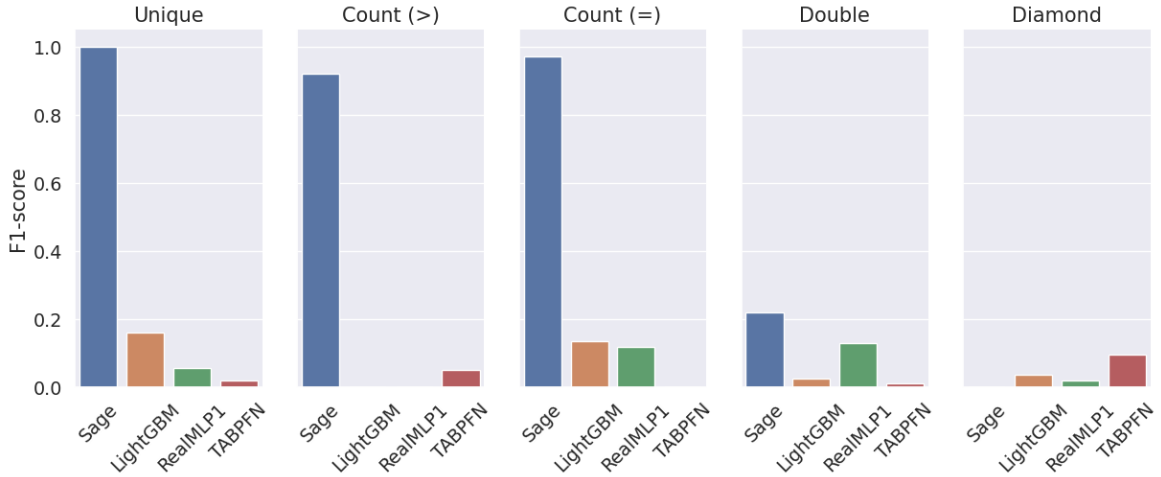


Figure 6. F1 score of each model in the stress-set data. GNN presents good performance on 3 of the 5 tasks, even when the data does not allow learning shortcuts.

Table 10. Performance on original vs. cleaned retail data (Unique, Count). $\Delta = \text{Clean} - \text{Orig}$.

Model	$t_1: \text{unique}$			$t_2: \text{count}(>)$			$t_2: \text{count}(=)$		
	Orig	Clean	Δ	Orig	Clean	Δ	Orig	Clean	Δ
<i>F1-score</i>									
GNN (SAGE)	0.988	0.989	+0.001	0.967	0.997	+0.030	0.171	1.000	+0.829
LightGBM	0.190	0.190	+0.000	0.000	0.000	+0.000	0.027	0.027	+0.000
realMLP	0.190	0.191	+0.001	0.881	0.885	+0.004	0.027	0.027	+0.000
TabPFN	0.404	0.406	+0.002	0.001	0.001	-0.000	0.023	0.019	-0.004
<i>ROC-AUC</i>									
GNN (SAGE)	0.998	0.999	+0.001	0.999	0.999	+0.000	0.903	1.000	+0.097
LightGBM	0.570	0.540	-0.030	0.500	0.000	-0.500	0.500	0.500	+0.000
realMLP	0.853	0.708	-0.145	0.929	0.882	-0.047	0.477	0.570	+0.093
TabPFN	0.793	0.802	+0.009	0.827	0.561	-0.266	0.758	0.716	-0.042

Tables 10 and 11 show both F1 and ROC-AUC performance for the 4 logical tasks, using the original retail transactions data and the simplified (or clean) version of it. We observe that the GNN maintains its performance for almost every task, with the exception of Counting with equality, where it lifts significantly.

G.3. Case study

G.3.1. FEATURE IMPORTANCE OF DIFFERENT MODELS

Tabular only model. We train a tabular-only model using AutoGluon’s tree-based ensemble methods and evaluate feature importance via permutation importance with respect to the F1 score. As shown in Figure 7, text-derived fields dominate the model’s predictive performance, while most structured metadata features exhibit smaller or statistically indistinguishable effects. Several features yield near-zero or negative importance, indicating limited or potentially detrimental contribution to model performance.

Tabular + NFA (intra-table). A similar tree-based tabular model, trained and ensembled with Autogluon is applied over the tabular data with extra features coming from the time-aware tabular neighbor feature aggregation procedure (Appendix E). Figure 8 shows the most important 15 features. The top features are shared with the tabular only method, but from the 15 most important features, 6 correspond to newly aggregated features.

Table 11. Performance on original vs. cleaned retail data (Double, Diamond). $\Delta = \text{Clean} - \text{Orig}$.

Model	$t_3: \text{double condition}$			$t_4: \text{diamond}$		
	Orig	Clean	Δ	Orig	Clean	Δ
<i>F1-score</i>						
GNN (SAGE)	0.863	0.855	-0.008	0.251	0.249	-0.002
LightGBM	0.815	0.672	-0.143	0.199	0.087	-0.112
realMLP	0.000	0.819	+0.819	0.139	0.169	+0.030
TabPFN	0.005	0.005	+0.000	0.007	0.007	+0.000
<i>ROC-AUC</i>						
GNN (SAGE)	0.910	0.908	-0.002	0.807	0.836	+0.029
LightGBM	0.847	0.420	-0.427	0.821	0.769	-0.052
realMLP	0.703	0.827	+0.124	0.792	0.743	-0.049
TabPFN	0.463	0.380	-0.083			
	0.659	0.560	-0.099			

Tabular + GNN embeddings (intra-table). Figure 9 shows the 15 most important features for the tabular tree-based model trained on the tabular data augmented with embeddings obtained from training a GNN over the incidence graph of the table. Out of the 15 most relevant features, 9 corresponds to GNN embeddings generated features, showing how the model is actually using them to predict. At the top, there still remain the free text features from the data.

Tabular + GNN embeddings (relational entity graph), Figure 10 shows the 15 most important features for the tabular tree-based model trained on the tabular data augmented with embeddings obtained from training a GNN over the relational entity graph derived from the full relational database (Figure 4). Out of the 15 most relevant features, 7 corresponds to GNN embeddings generated features. Moreover, its interesting to see how more of the original tabular features place at the top when the intra-structure of the table is not exposed in the graph (and therefore not properly captured in the GNN embeddings)

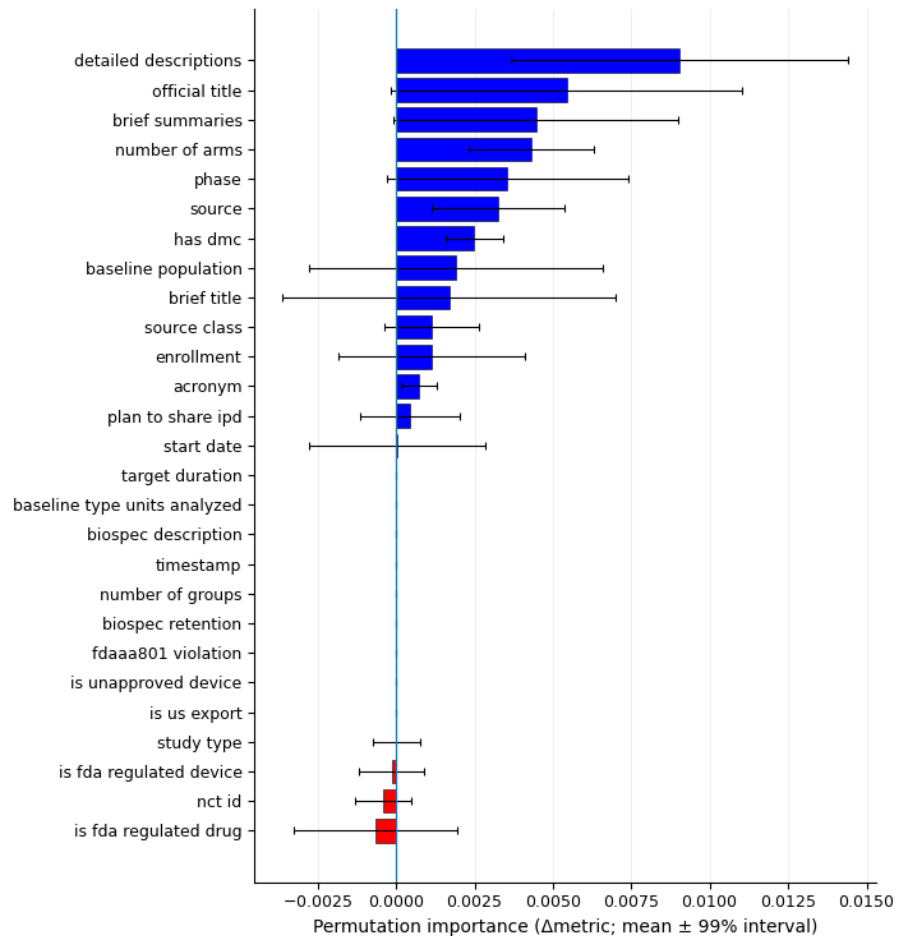


Figure 7. Permutation feature importance based on ROC-AUC score for the AutoGluon tabular model. Bars show the mean change in F1 score ($\Delta F1$) under feature permutation, with 99% confidence intervals from repeated shuffles. Positive values indicate performance degradation, while negative values indicate improved performance after permutation.

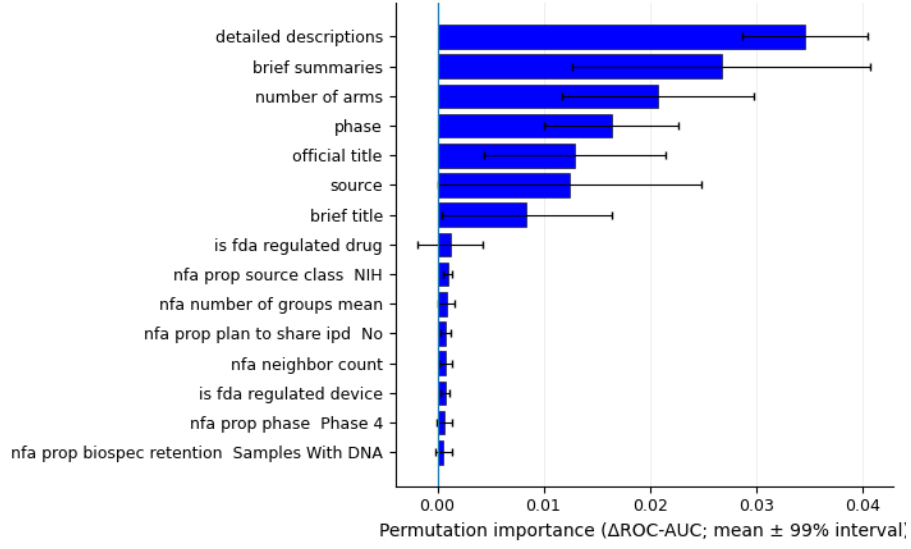


Figure 8. Permutation feature importance based on ROC-AUC score for the AutoGluon tabular model with tabular time-aware neighbor feature aggregation features. Bars show the mean change in ROC-AUC score (Δ ROC-AUC) under feature permutation, with 99% confidence intervals from repeated shuffles. Trimmed to most relevant 15 attributes.

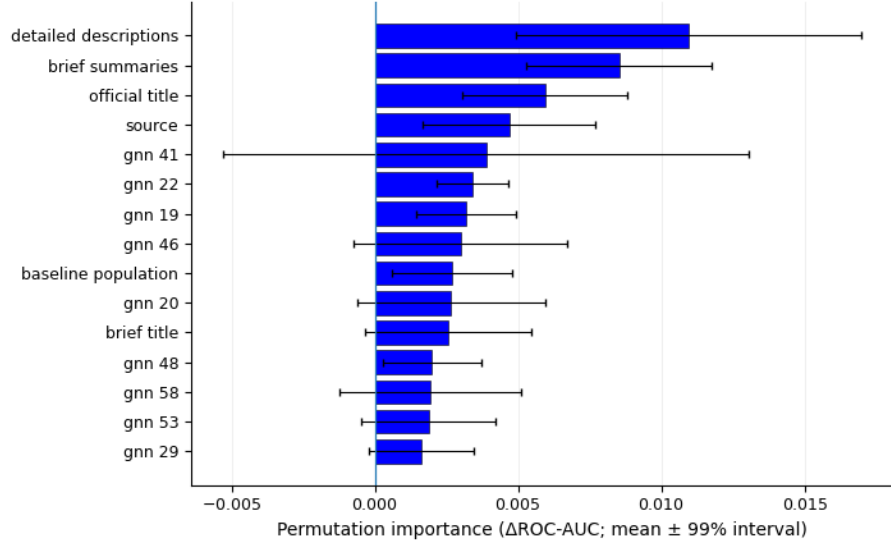


Figure 9. Permutation feature importance based on ROC-AUC score for the AutoGluon tabular model augmented with embeddings from a GNN trained on the incident graph from the table. Bars show the mean change in ROC-AUC score (Δ ROC-AUC) under feature permutation, with 99% confidence intervals from repeated shuffles. Trimmed to most relevant 15 attributes. Important to note that out of the 15 most important attributes, 9 correspond to GNN embeddings.

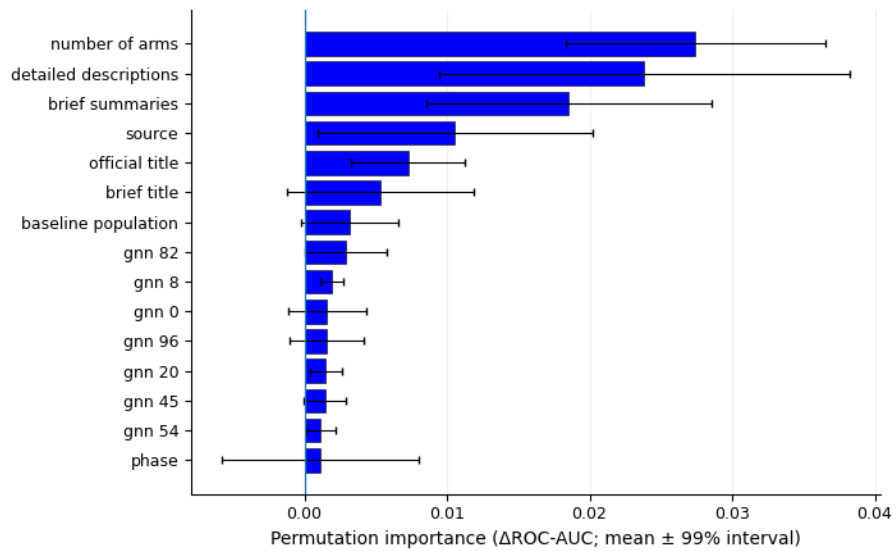


Figure 10. Permutation feature importance based on ROC-AUC score for the AutoGluon tabular model augmented with embeddings from a GNN trained on the relational entity graph from the entire database. Bars show the mean change in ROC-AUC score (Δ ROC-AUC) under feature permutation, with 99% confidence intervals from repeated shuffles. Trimmed to most relevant 15 attributes. Important to note that out of the 15 most important attributes, 7 correspond to GNN embeddings.